Feasibility Research on Dark Energy Signal Regions at the LHC

Zhiying Li[1;1], supervisors : Michaela Queitsch-Maitland and James Ferrando
[1] Lund University, Sweden

Key words: dark energy, top squark, dark matter

1 Introductions

The existence of Dark Matter was first suggested in 1930s to explain astronomical observations about the accelerating expansion of the universe and later on the gravitational lensing effect also added to the evidences. Here "dark" describes they are different from the matter we know of. [1] According to the observations of our mass-energy universe, about 68% is dark energy and 27% is dark matter. The known energy and matter only take up about 5% of the whole universe. Many theoretical models have been forwarded and experimental searches have been conducted to detect these unknown particles ever since. One of the models is the Horndeski model, describing a scalar field coupled to gravity for dark energy. It is also expected that dark energy scalar to couple with matter. In this model, the collider phenomenology of the operators can be expressed as Equation (1). The c_i here are the Wilson coefficients and the orders are limited to the lowest non-trivial orders in each operator series. [1]

$$L_{BSM} = L_{SM} + \sum_i C_i L_i + \frac{1}{2} m_\phi^2 \phi^2 \tag{1}$$

There are also suggested new particles. As for supersymmetry (SUSY) models, the basic idea is for fermions and bosons, they should both have a symmetric particle in the other kind, being their supersymmetry, like for a top quark its supersymmetry partner would be a "stop". Charginos are what charge the supersymmetry particles and a wino is a SUSY partner of a W boson while a bino is the SUSY partner of U(1) gauge field related to weak hypercharge. Similar models on dark matter and supersymmetry particles were also developed and studied. Like for the lightest supersymmetric particle (LSP), there are charginos and neutralinos as the mass eigenstates of charged and neutral SUSY partners of Higgs and electroweak gauge bosons like higgisinos, winos and binos. [2] For DM model used, it also has a scalar mediator. In the samples of this research the lightest neutralino is taken as the LSP. People hope that the LHC, the current largest collider for high energy particle physics, would have some signals indicating these unknown particles.

Based on these model and idea, modified phenomenology of LHC processes which are possibly dark energy, dark matter and SUSY interactions are surveyed and related simulations are produced with MadGraph tools, as detailed in Ref. [2] and [3]. The Feynman diagrams focused on are given in Fig. 1. The first two operators as described in (1), with coefficients C_1 and C_2, are the main dark energy modes mainly studied here in this research. In this research DE C_1 will stand for C_1 equals to1 and other C_is are 0, and C_2 is for $C_2 = 1$ and others are 0. For DE (Dark Energy) mode, the DE particles are the decay products given as ϕ_{new}. From the Feynman diagrams, it is clear to see that the expected signals from the ATLAS detector should be t and $\bar{t}$, which would result in jets, leptons and neutrinos. What is focused on here are the one-lepton reactions. It is a natural idea to study what kind of selections are most efficient for selecting the interesting signals. The ATLAS collaboration has already searched for SUSY particles in scenarios like pure bino LSP model, wino NLSP model and Higgsino LSP model [2]. The event selection used for the previous search will be applied in this research. A series of cut selections optimised to maximum the significance for certain samples are signal regions. There are also signal regions optimised for the Dark Matter samples we would like to test.

The main idea for this research is to determine the optimised selection for simulated dark energy samples and compare the results with dark matter and super symmetry particle samples, which results will be given in following sections. By studying these simulated signals we can have a basic idea of these models and know what to expect from the real ATLAS data, which makes this research important for following studies on these models. The simulation signal generation is done with athena MadGraph v2.4.3 [3], settings as authors recommended. Most of the studies are done with MC (Monte Carlo) Truth level data and we also generated some full simulated data to compare these results. Cross sections, as well as events passing each selection, are discussed. Significances of each signal region for Dark Energy are also studied and results given. Some variables are often used as discriminators in selections. They are deemed important because of their usage in these signal regions of interest.

---

1) E-mail: zh6542li-s@student.lu.se

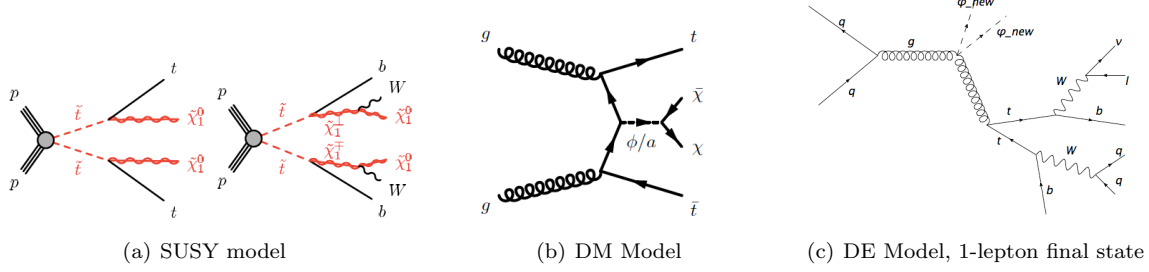(a) SUSY model   (b) DM Model   (c) DE Model, 1-lepton final state

Fig. 1. Main Feynman diagrams used in this research, included supersymmetry, dark matter and dark energy models.

2 Signal Regions and Variable Distributions

First, plots for DE C_1 model, DE C_2 model, SUSY model and DM model were made (with and without selections) over some potential discriminating variables mentioned above to compare their differences. By comparing these signals he similarities and differences between the samples can be seen, which might indicate proper signal regions for dark energy particles. Several existing selections of potential interest are chosen to test these samples. The chosen selections applied here are tN_high selection, tN_med, DM_high, DM_low and bC2x_diag selection, detailed in Ref. [2]. Their detailed cuts are given in Table 1. These selections were developed first for other signal detections for example, tN selections are for top neutralino and low, med and high indicates the targeted stop mass range. For tN_med, the optimised stop mass is 600 GeV and for tN_high it is 1000 GeV. In this way bC selections are meant for "bottom chargino", and 2x denotes the mass relation in the model. It is also optimised to look at stop mass of 600 GeV. DM labels spin-0 mediator scenario, and high and low give the mediator masses. DM_high is optimised for mediator mass of 300 GeV and DM_low goes for 20 GeV mediator mass. But DM_low also used 300 mediator mass for data collection due to 20 GeV samples were not ready at that time. Since this simulation is still Monte-Carlo truth level, no cuts can be applied on parameters τ-veto and mass of reclustered W bosons even if they are required by some SRs (signal regions). In Table 1, selection cuts on high-E_T^{miss} and number of jets and b-tags are shared by many signal regions, those are thought as preselections. E_T^{miss} describes the energy loss and is a very important variable in these selections, as it can cut of most of the events. Cut efficiency plots can be found in Appendix.

Table 1. Selection Cuts for Signal Regions

cut information	tN_med	tN_high	DM_low	DM_high	bC2x_diag
preselection	high-E_T^{miss} preselection				
Number of (jets, b-tags)	$(\geqslant 4, \geqslant 1)$	$(\geqslant 4, \geqslant 1)$	$(\geqslant 4, \geqslant 1)$	$(\geqslant 4, \geqslant 1)$	$(\geqslant 4, \geqslant 2)$
Jet p_T [GeV]	$> (60, 50, 40, 40)$	$> (100,80,50,30)$	$> (120, 85, 65, 25)$	$> (125, 75, 65, 25)$	$> (75, 75, 75, 30)$
b - tagged jet p_T [GeV]	–	–	>60	> 25	$> (30, 30)$
E_T^{miss} [GeV]	> 250	> 550	>320	>380	> 230
$E_{T,\perp}^{miss}$ [GeV]	> 230	–	–	–	–
$H_{T,sig}^{miss}$	> 14	> 27	> 14	–	> 13
m_T [GeV]	> 160		> 170	> 225	> 180
am_{T2} [GeV]	> 175		> 160	> 190	> 175
$m_{top}^{reclustered}$ [GeV]	> 150	> 130	> 130	> 130	–
$\Delta R(b,l)$	< 2.0		–	–	
$\|\Delta\phi\|(j_{1,2},p_T^{miss})$	> 0.4				> 0.4
$\|\Delta\phi(jet_i,p_T^{miss})\|$	–	–	> 1.0	> 1.0	> 0.7 (i = 1,2)
$\Delta\phi(p_T^{miss},l)$	–	–	> 1.2	> 1.2	–
m_{T2}^τ based τ-veto [GeV]	MC Truth Level cannot apply, needed for all				
$m_W^{reclustered}$ [GeV]	MC Truth Level cannot apply, needed for bC2x				

For MC_truth, weight information needs to be added when calculating the expected event number for the ATLAS Run2 dataset. The weight is considered and the integrated luminosity is assumed to be 36.5 fb^{-1}. The weighted distributions for some important variables are given in following figures. After preselection cuts (number of jet at least 4, at least 1 bjet and 1 lepton), the distributions of some selection-related variables are given in Fig. 2. The upper plots show distribution and the lower ones show how different these variables are in different samples (ratio panels). There are also similar plots for samples after different selections. For example, after the tN_high selection,

(a) met (transverse momentum loss)

(b) leading jet pt

(c) angular differences between missing energy and lepton
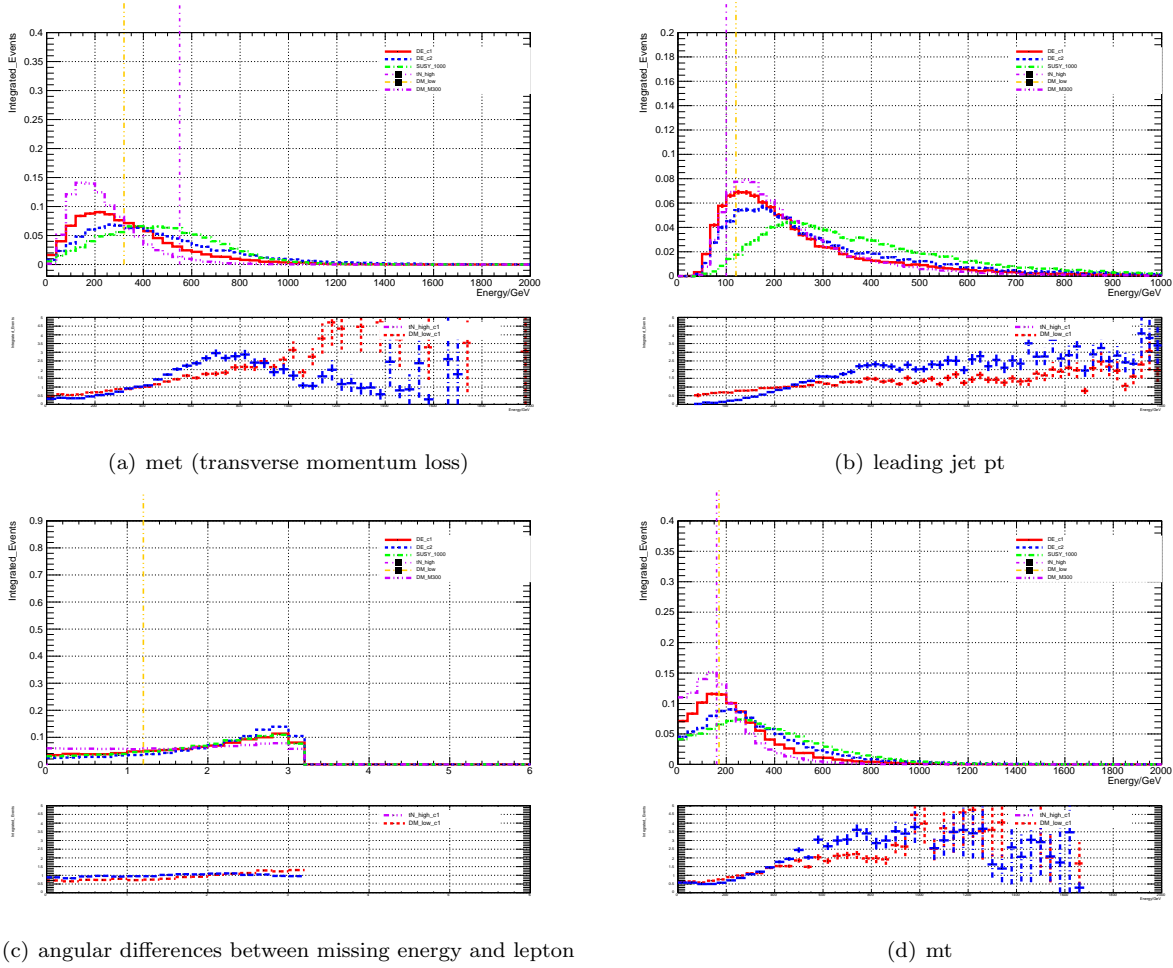

(d) mt

Fig. 2.   Some characteristic variable distributions at preselection level and comparison between different samples.

distributions are shown in Fig. 3 and after DM_high, the variables are shown in Fig. 4. With these plots the behaviour of variables used in selections can be studied and have some idea of how similar or different are these samples. It can be seen that C_1 (M scale at 600 GeV) and Dark Matter (mediator mass at 300 GeV) sample are more similar than others.

3   Results

3.1   M scale Related Studies

The cross sections for DE production were obtained from Madgraph. The values are shown in Table 4. To have a more direct idea of how they look, the cross section dependence on M scale is given in Fig. 5. As can be seen here, the cross section decreases as the M scale increases. The potential variable distribution shape changes as M scale changes were also studied and no significant differences were spotted. Some exapmles are given in Appendix. As a result, it should be safe to say that the change in event number is proportional to cross sections and is not influenced by M scales.

With weight information accounted for, the calculate expected event number can also be calculated from datasets within different selection ranges. For tN_high and DM_high selection, the expected event numbers and simulated particle mass relations are in Fig. 6. The exact numbers of events for each sample to pass each selections can also be obtained, the results given in Table 3.
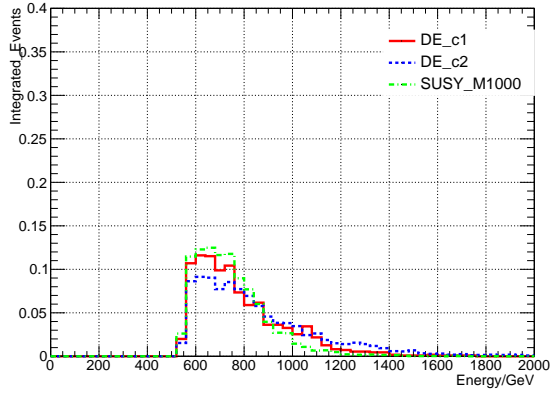
(a) met (transverse momentum loss)
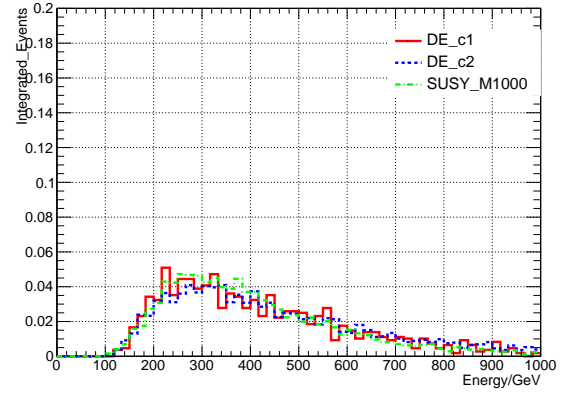
(b) leading jet pt
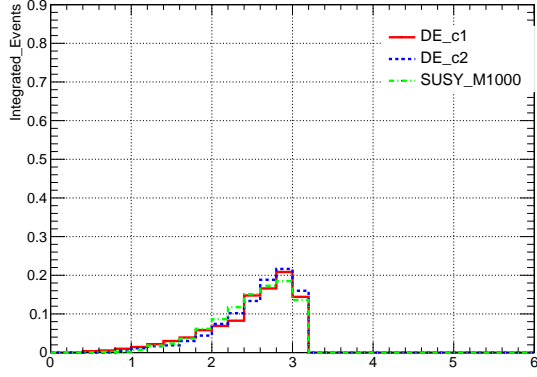
(c) angular differences between missing energy and lepton
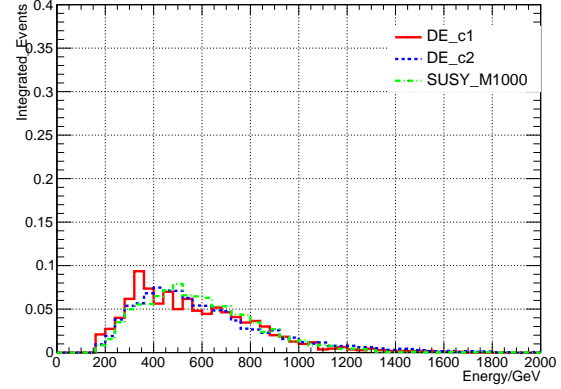
(d) mt

Fig. 3. Some characteristic variable distributions after tN_high selection and comparison between different samples.

(a) met (transverse momentum loss)

(b) leading jet pt

(c) angular differences between missing energy and lepton

(d) mt
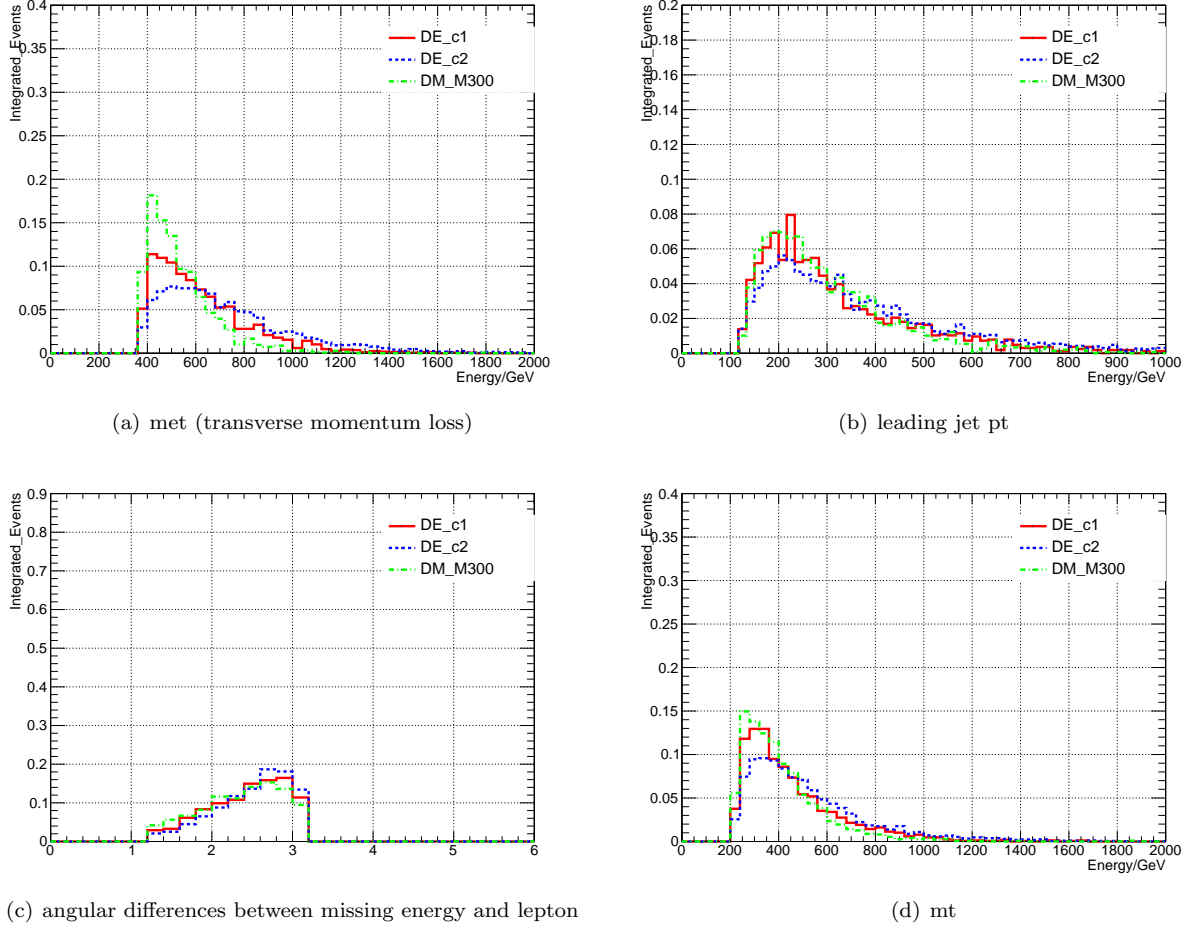
Fig. 4. Some characteristic variable distributions after DM_high selection and comparison between different samples.
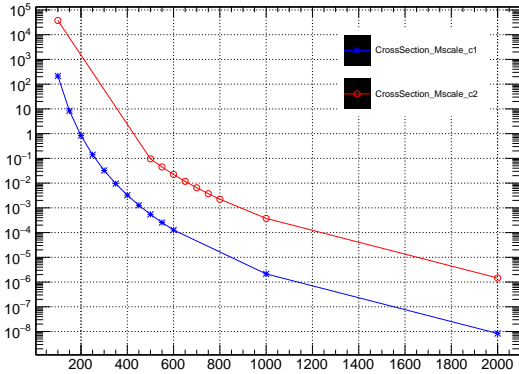
Fig. 5. Cross section and M scale relations for C_1 and C_2. As can be seen, the cross section decreases as M scale increases.
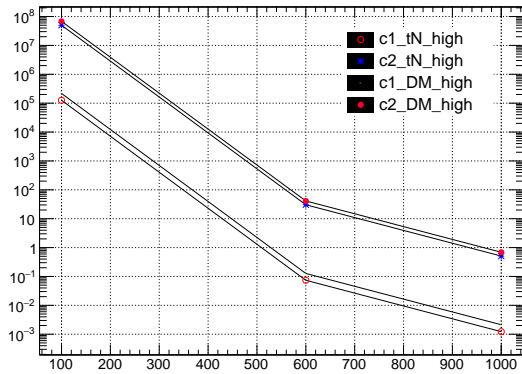
Fig. 6. Number of events of C_1 and C_2 samples passing tN_high and DM_high selections. The relation is consistent with the cross section relation.

Table 2.   Cross Section numbers for C_1 and C_2 at different M scale (new one)

M scale (GeV)	DE_C_1 (pb)	DE_C_2 (pb)
100	213.3	37430
150	8.321	-
200	0.8331	-
250	0.1398	-
300	0.03251	-
350	9.47e-3	-
400	3.254e-3	-
450	1.268e-3	-
500	5.46e-4	0.09583
550	2.547e-4	0.04479
600	1.27e-4	0.02229
650	-	0.01175
700	-	6.494e-3
750	-	3.739e-3
800	-	2.231e-3
1000	2.133e-6	3.743e-4
2000	8.331e-9	1.462e-6

Table 3.   Event counts and percentage of passing certain selection for each sample at M scale of 1000 GeV, MC Truth Level

Selection	DE_C_1 number(percentage)	DE_C_2 number(percentage)	DM number(percentage)	SUSY number(percentage)
no_selection	1.4595e-2	2.2873	5.84	62.78
DM_high	1.284e-3 (0.236%)	4.626e-1 (13.26%)	0.3325 (4.25%)	13.61 (16.65%)
tN_high	8.382e-4 (4.3%)	4.314e-1 (12.37%)	0.19047 (2.4%)	11.62 (14.22%)
DM_low	1.5625e-3 (8.06%)	5.0687e-1 (14.53%)	0.4003 (5.12%)	14.8382 (18.17%)
tN_med	1.885e-3 (9.73%)	6.8824e-1 (19.72%)	0.52944 (6.77%)	20.2683 (24.80%)
bC2x_diag	2.1675e-3 (11.18%)	6.0168e-1 (17.29%)	0.5940 (7.59%)	21.843 (26.73%)

Since the M scale does not change the variable distribution but just changes the cross section, the expected events for other M scales can be obtained by scaling the cross section. The scaling equation is shown in (2). The results shown in Table 4 and Table 5. These numbers can be used in further studies on this model and comparing the performance of MC Truth Level simulation with full simulated detector level simulation, the results of which will be shown later in this document.

$$N_{M=x} = N_{M=1000GeV} * \frac{\sigma_{M=x}}{\sigma_{M=1000GeV}} \tag{2}$$

Table 4.   DE C_1 event counts of passing certain selection for different M scales

M scale (GeV)	no selection	DM_high	DM_low	tN_high	tN_med	bC2x_diag
200	5700	501.5	610.28	327.38	736.24	846.57
250	956.58	84.16	102.41	54.94	123.55	142.06
300	222.45	19.57	23.81	12.78	28.73	33.04
350	64.80	5.7	6.93	3.72	8.37	9.62
400	22.27	1.96	2.38	1.28	2.88	3.31
450	8.68	0.76	0.93	0.50	1.12	1.29
500	3.74	0.33	0.40	0.214	0.48	0.555
550	1.74	0.153	0.187	0.100	0.225	0.259
600	0.869	0.076	0.093	0.050	0.112	0.129
1000	0.0146	0.00128	0.001563	0.00084	0.00189	0.00217
2000	5.57e-5	5 e-6	6e-6	3e-6	7e-6	8e-6

Table 5.   DE C_2 event counts of passing certain selection for different M scales

M scale (GeV)	no selection	DM_high	DM_low	tN_high	tN_med	bC2x_diag
500	636.81	118.44	129.77	110.45	176.21	154.04
550	297.64	55.36	60.65	51.62	82.36	72
600	148.12	27.55	30.18	25.69	40.99	35.83
650	78.08	14.52	15.91	13.54	21.6	18.88
700	43.15	8.03	8.79	7.48	11.94	10.44
750	24.85	4.62	5.06	4.31	6.88	6.01
800	14.83	2.76	3.02	2.57	4.10	3.59
1000	2.49	0.46	0.51	0.43	0.69	0.60
2000	9.715e-3	1.807e-3	1.98e-3	1.685e-3	2.69e-3	2.35e-3
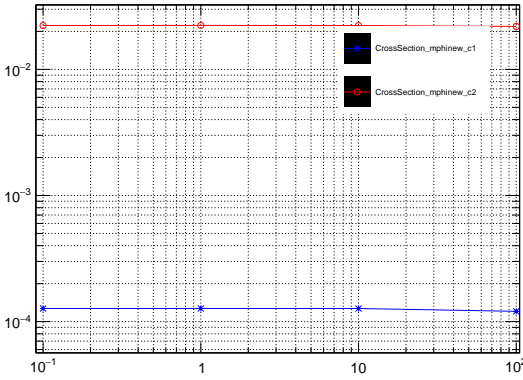
Fig. 7.   Cross section and M scale relations for c1 and c2. As can be seen, the cross section decreases as M scale increases. x axis : M scale, y axis : cross section (pb)
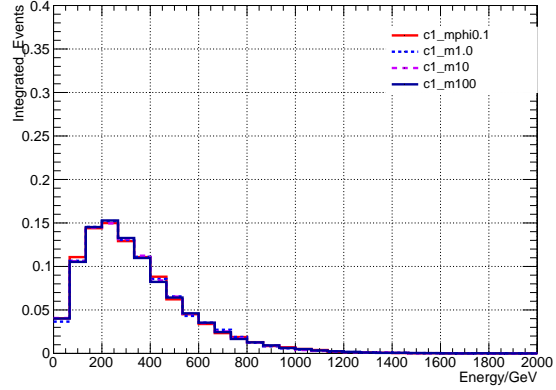
Fig. 8.   Number of events of c1 and c2 samples passing tN_high and DM_high selections. The relation is consistent with the cross section relation.

3.2   Mphi Related Studies

Another natural idea is to study the change of mass of the final state phi particles, which are the "new physics particles" in the models we are studying. Mphi will be used as short of mass of phi in later discussions. Samples with different mphi were made to study its effect on the cross section. Since the phi particles are invisible to detectors and the mass is comparatively small regarding to the M scale, we do not expect to see it having large influence on cross sections when mass of phi particles much smaller than the mediator mass. The actual simulated results agreed with this expectation, as is shown in Fig. 7. Another possible idea would be to see if the phi mass would influence the parameter distribution shapes. Tests are also done to test this idea but these results are also identical. An example plot (met, transverse momentum loss) is given in Fig. 8.

These results show that at least when the mass of the new phi particle is much smaller than the M scale, the influence of mphi on cross sections and variable distributions are negligible, which is also expected.

3.3   Comparison between Detector Level and Particle Level Simulations

The results mentioned above are all at MC Truth Level, and it is very important to see if they match with samples at fully simulated detector level. To achieve this, detector level samples were made and similar results in event numbers can be obtained by applying the similar selections to them. The samples are C_1 and C_2 at M scale of 600 GeV, supersymmetry top (stop) at 1000 GeV and 600 GeV, DM at mediator mass of 20 and 300 GeV, as shown in Table 6. As can be found, the event numbers passing each selection are usually higher than MC Truth Level, which could be understood since some background will be inevitable involved when it comes to detector level simulations. These results basically match with MC Truth Level data results, as were expected. Significances can also be studied with these data and that will be detailed in the significance studies part.

Table 6. Event counts of passing certain selection for samples at fully simulated detector level

Selection	DE_c2_M600	stop_tN_1000	stop_tN_600	DM_M20	DM_M300
no_selection	89.90	35.10	757.43	18056	143.5
tN_high	14.693	6.11	1.127	3.068	1.548
tN_med	21.28	9.69	32.87	29.52	7.36
DM_low	15.4	6.8	13.70	17.70	4.88
DM_high	14.3	6.38	5.01	9.97	3.56
bC2x_diag	10.47	5.519	18.31	19.00	4.42

Table 7. significance at 600 GeV M scale for DE_C_1 and DE_C_2 samples at MC Truth Level

-	tN_med	tN_high	bC2x_diag	DM_low	DM_high
Optimised Model	stop_tN_600_300	stop_tN_1000_1	stop_tN_600_300	DM_scalar_p300_c1	DM_scalar_p300_c1
N_{model}(truth)	68.42	11.62	66.48	8.13	5.41
N_{model}(detector)	32.87	6.11	18.31	4.88	3.56
N_b DE	36.08	3.99	17.37	13.42	7.48
N_s DE_c1	5.38e-2	2.63e-2	3.55e-2	5.58e-2	5.00e-2
DE_c1 (significance)	4.35e-3	1.13e-2	5.32e-3	1.03e-2	1.41e-2
N_s DE_c2	19.69	13.51	9.87	18.12	18.13
DE_c2 (significance)	1.59	5.8	1.48	3.33	5.12

3.4 Significance Studies

The expected significances is a good metric to judge the performance of different selections. A good significance would be obtained by reducing the background as much as possible whilst still keeping a good quantity of signal. A lot of time was spent studying the significances of the existing selections on DE C_1 and C_2, trying to find a best signal region for these models. Since the significance needs to be studied at detector level, and at that time detector level data was not ready for some samples, so scaling was applied to get the estimated significance. First estimate the number of signal by scalings (3) and it is assumed that the uncertainty of the background to be 0.3 times of the background event number, then use (4) to calculate significance, which b stands for backgrounds. The results are summarised in Table 7. In Table 7 it gives the samples for which the signal regions are optimised, and also the total background.

$$N_s^{det} \sim N_s^{det}(optimised) * \frac{N_s^{truth}(DE)}{N_s^{truth}(optimised)} \quad (3)$$

$$sig = \frac{N_s}{\sqrt{b + (0.3*b)^2}} \quad (4)$$

From the table it can be seen that tN_high gives highest significance for C_2 and DM_high gives best significance to C_1, while the significance difference is quite small for these two. So the significance - M scale relation for C_1 and C_2 was studied and this result is given in Fig. 9. As can be seen here, DM_high and tN_high lines are very close and they are better than other signal regions. Also it is clear that these signal regions are much more sensitive to C_2 than C_1, which is also as expected since the C_2 variable shapes are closer to the existing samples than C_1. Since other detector level simulations were ready by then, the significances at detector level results are obtained as well. The significance calculations are shown in Table 8. Fig. 10 is plotting them with M scale. Comparing results of these with the MC Truth Level, it can be seen that they agree with each other and both have tN_high as the best significance signal region for C_2 samples. While at detector level, tN_high gives best significance for C_1 instead of DM_high. The reason of this might lie in the differences of physics between stop and DM, C_1 is more close to DM M300 than it is to stop M1000. This could lead to the scaling which was applied to estimate the detector level number from MC Truth numbers not performing very well. Detector level simulation shows that C_1 performances at tN_high better than expected with MC Truth Level but in DM_high region it is not doing that good. But the difference is fairly small and all significances for c1 at these signal regions are small. So it is understandable if a "rough" estimate applied in something small, there might be influences on the actual results.
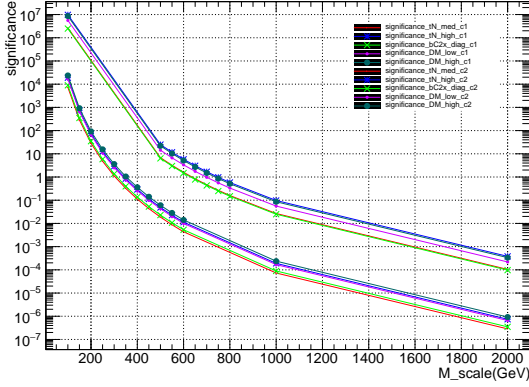
Fig. 9. MC Truth Level (Particle Level). Significance relation with M scale for different signal regions, C_1 and C_2.
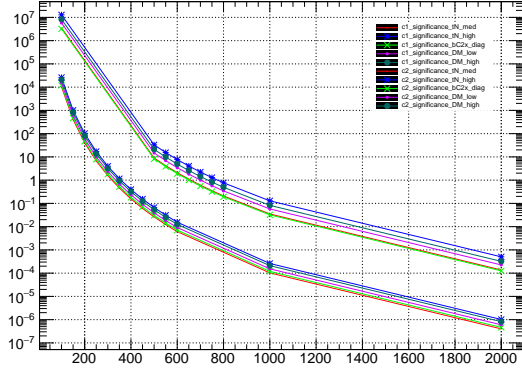
Fig. 10. Detector Level Simulation. Significance relation with M scale for different signal regions, C_1 and C_2 .

Table 8. significance at 600 GeV M scale for DE_C_1 and DE_C_2 samples at detector level.

-	tN_med	tN_high	bC2x_diag	DM_low	DM_high
N_b	36.08	3.99	17.37	13.42	7.48
N_s DE_c2	25.88	17.86	12.73	18.73	17.24
DE_c2 (significance)	2.09	7.67	1.91	3.44	4.91
N_s DE_c1	7.58e-2	3.6e-2	4.73e-2	4.98e-2	4.415e-2
DE_c1 (significance)	6.12e-03	1.55e-2	7.09e-3	9.156e-3	1.25e-2

143

After looking at the significance of the existing signal regions, C_1 and C_2 have different best fit signal regions, but since C_2 is the more sensitive one here, and tN_high already has a very good significance for C_2, it may be a good start to look at C_2 first. Another thing tried is if optimisation on the signal region (tN_high) is possible to get another signal region optimised specially for Dark Energy samples. Since tN_high was not originally optimised for DE samples, attempts to optimise this signal region specifically for the dark energy samples were made. However, when studying the background samples, a problem arose that the number of events passing each selections are not identical with the results obtained from the flags within the simulation files. This could be an indication for some cut possibly left out for fully simulated samples when we simply apply the MC Truth cuts to fully simulated samples. This may require some further studies. Also there exist events passing the flags but not the cuts and they yield to very strange result (dr_bjet_lep $\sim$ 2.7, while the cut should actually be smaller than 2.0).

But the results of adjusting some parameters with the current cuts are still valid. They could improve this signal region for C_2 and are shown in Table 9. These results still can help with further optimisation when the problem with matching cuts and flags sorted out. As can be seen, the cuts can be loosened ton jet_p_T and tighten the cut on dr_bjet_lep (the distance between the jet and the lepton in the final state) are recommeded. Adding bjet_p_T cut to the tN_high signal region may also help optimise it for DE C_2 sample.

Table 9. Optimisations Tried and Related Results. The optimisations are based on tN_high signal region. Sample concerned : C_2 only, N_s here has been scaled to tN_high region detector level.

Cut change	N_b	N_s	significance
original tN_high	4.56	11.33	4.46
jet_pt (60,50,40,40) GeV	5.12	12.167	4.716
dr_bjet_lep < 1.5	3.529	9.9	4.59
bjet_pt > 60 GeV	4.124	10.87	4.59

9

4 Conclusion and Future Plans

This research gives variable distribution shape comparisons between different samples and cross sections at various M scale and mphi. Expected number of DE C_1 and DE C_2 events for signal regions can be estimated and significances studied. The main result with this research is the significance studies as finding and trying to improve the best significance signal region. For DE C_2, both at detector level and MC Truth Level, the best significance signal regions are both tN_high but for DE C_1 they have different results. Trying to set limits on these signal regions will help determine the final decisions.

With this progress so far, we also have several possible plans for future continuing studies. The first one could be checking where the differences between results from signal flags and applying cuts, and with current results, an optimised signal region specific to dark energy samples could be prompted. Or the same thing can be done by running over the optimisation codes to automatically find the best solution for DE samples. The second one can go down the path of studying other parameters like C_4, C_5 and C_7. In attempts to generate these data, some errors appeared and it was left for later. But with samples of C_4, C_5 and C_7, similar studies can be carried out and a more general view of this DE model will be given.

Thanks : I would like to thank the ATLAS Group at DESY and especially my supervisors, Michaela and James and also the DESY summer school program.

References

1 Philippe Brax, Clare Burrage, etc, LHC Signatures of Scalar Dark Energy, IPPP/16/31, DCPT /16/62

2 The ATLAS Collaboration, Search for top squark pair production in final states with one isolated lepton, jets, and missing transverse momentum using 36 fb^{-1} of $\sqrt{s} = 13$ TeV pp collision data with the ATLAS detector, ATLAS-CONF-Note-2017-037, 27th May, 2017

3 J. Alwall, R. Frederix, S. Frixione, etc. The automated computation of tree-level and next-to-leading order differential cross sections and their matching to parton shower simulations

5   Appendix

This section contains plots not included in the report itself. Old cross sections before the pdf change are also given here.

Table 10.   Old Cross Section numbers for c1 and c2 at different M scale

M scale (GeV)	DE_c1 (pb)	DE_c2 (pb)
100	391.126	30773
150	13.89	-
200	1.391	-
250	0.233	-
300	0.05427	-
350	0.01581	-
400	5.97e-3	-
450	2.327e-3	-
500	1.002e-3	7.878e-2
550	4.673e-4	3.675e-2
600	2.329e-4	0.0183217
650	-	9.657e-3
700	-	5.388e-3
750	-	0.003074
800	-	0.001834
1000	3.91276e-6	0.000307733
2000	1.528e-8	0.000001202
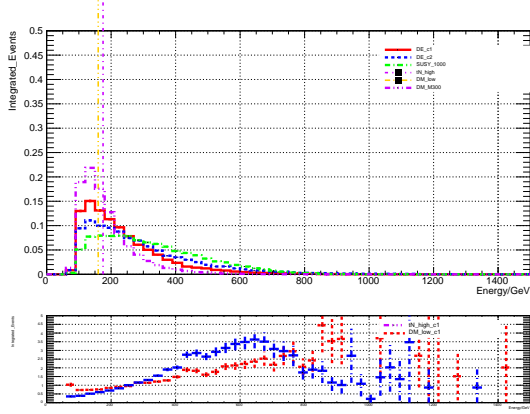
(a) amt2
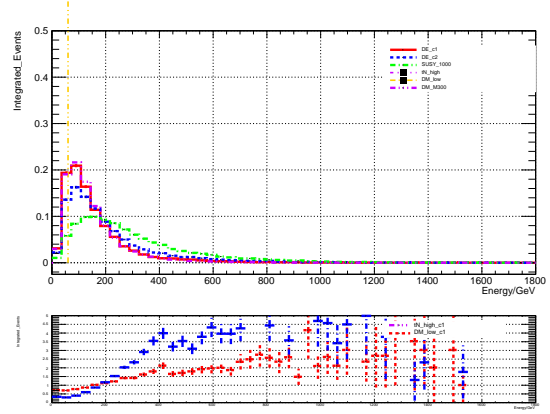
(b) bjet_pt
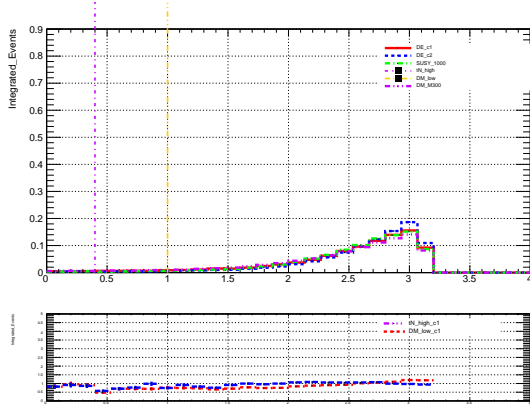
(c) dphi_jet0_ptmiss
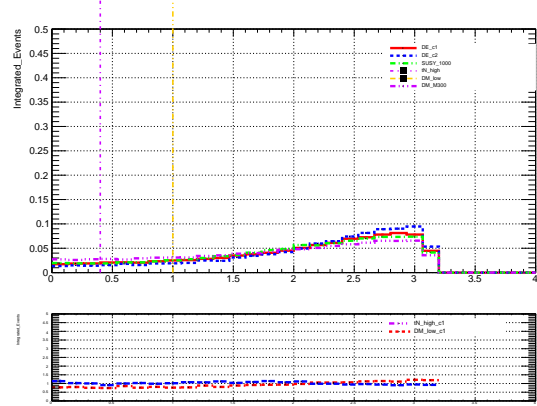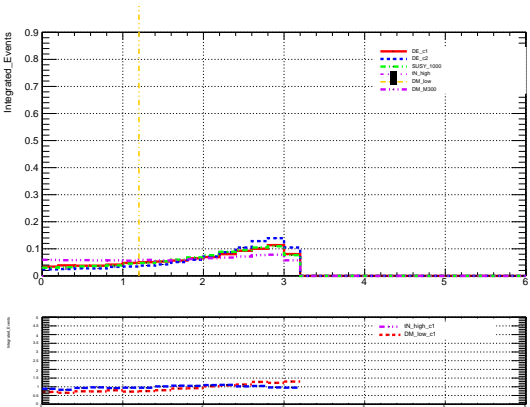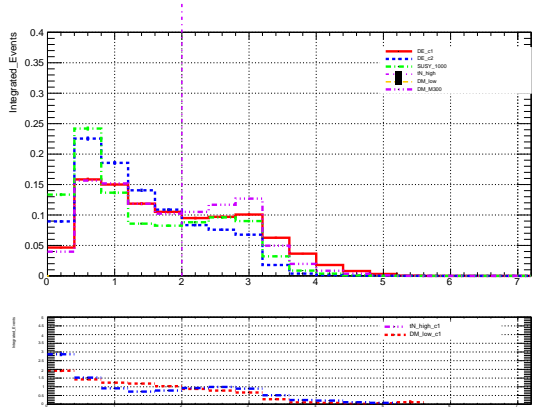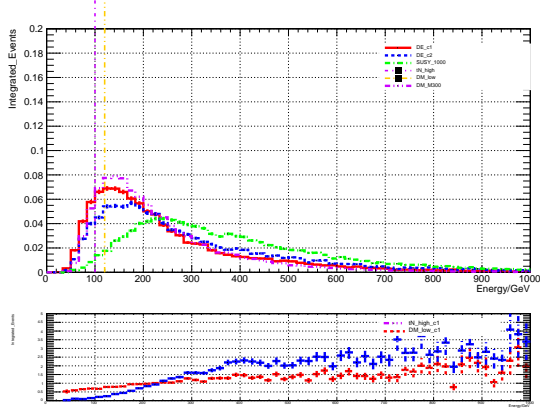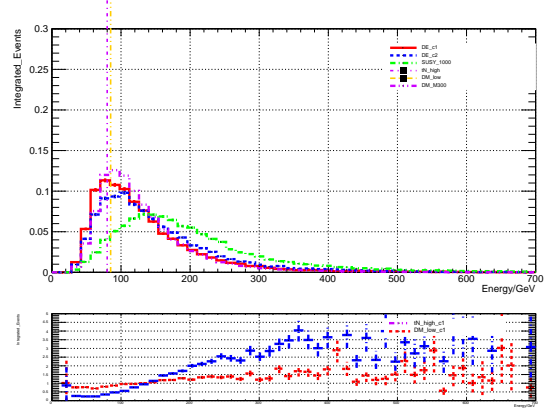
(d) dphi_jet1_ptmiss

(e) dphi_met_lep

(f) dr_bjet_lep

(g) leading_pt

(h) sub_leading_pt

(i) third_leading_pt

(j) fourth_leading_pt

(k) hadtop_mass

(l) ht_sig

(m) met

(n) mt
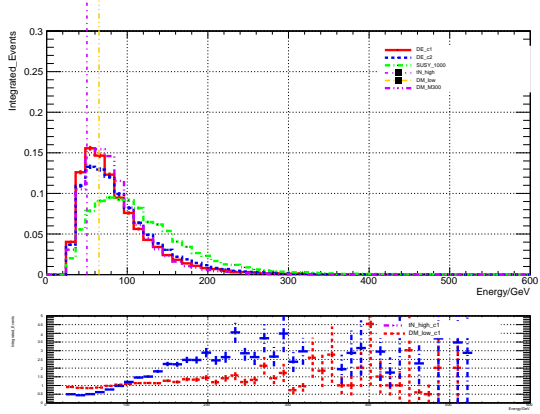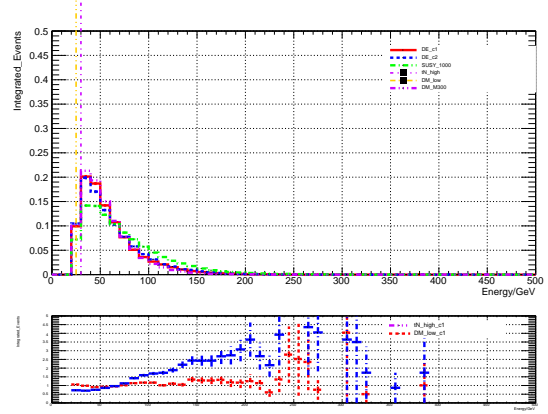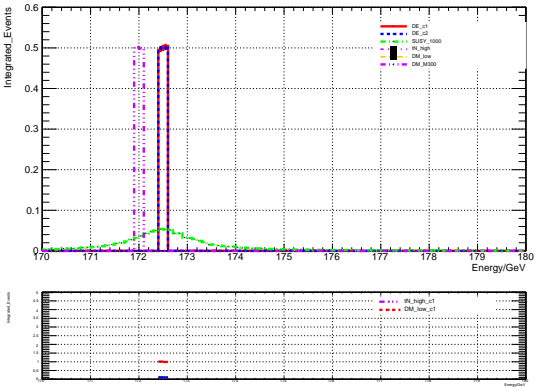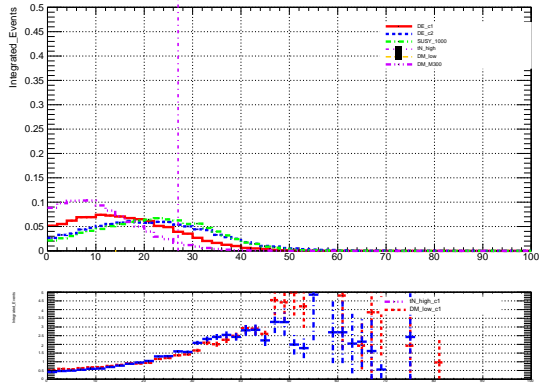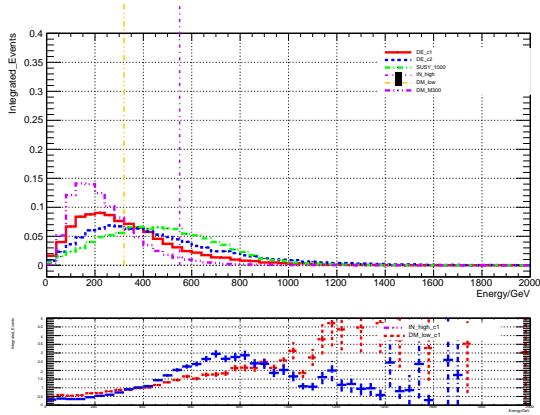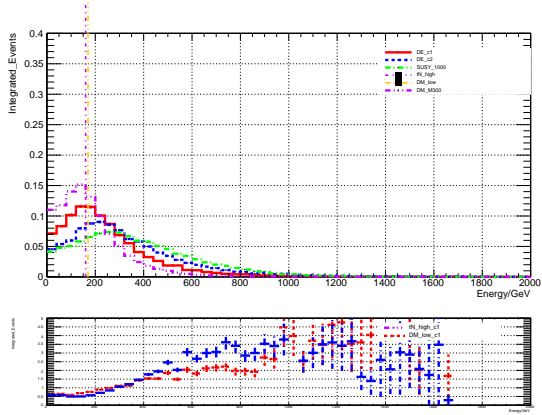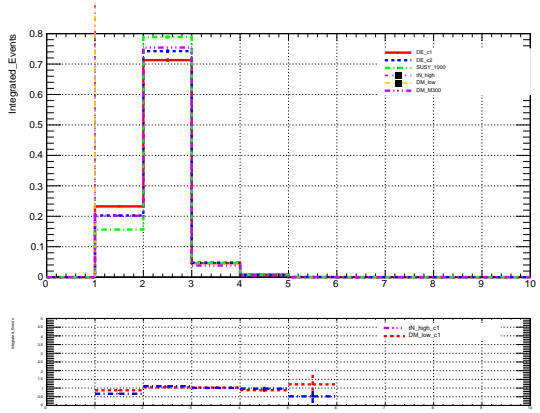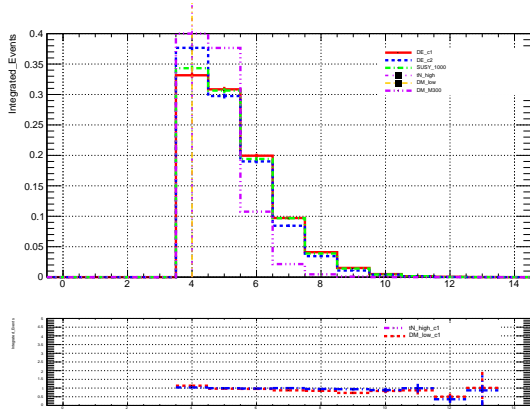
(o) n_bjet

(p) n_jet

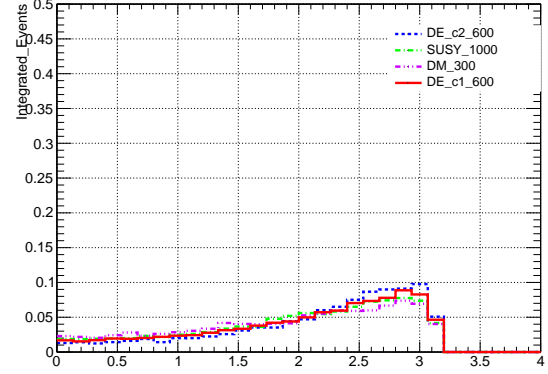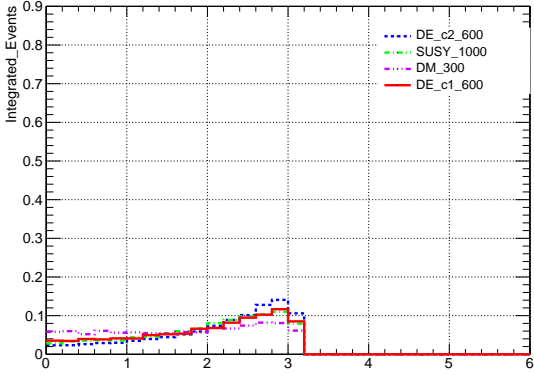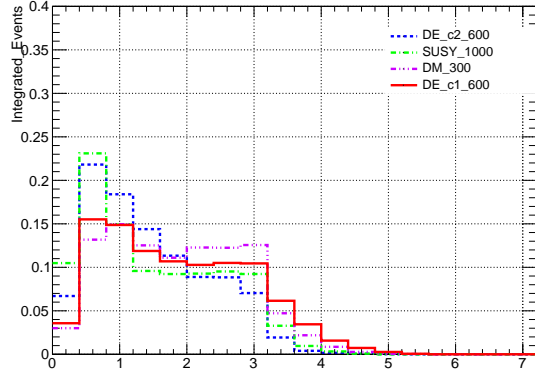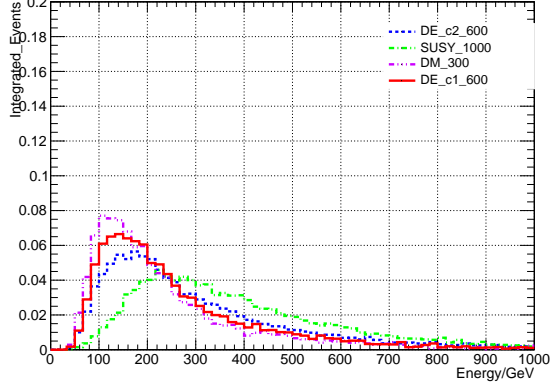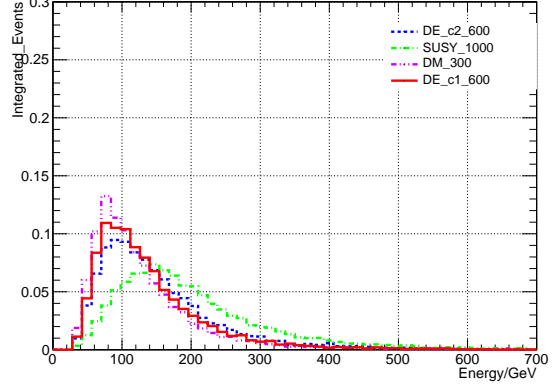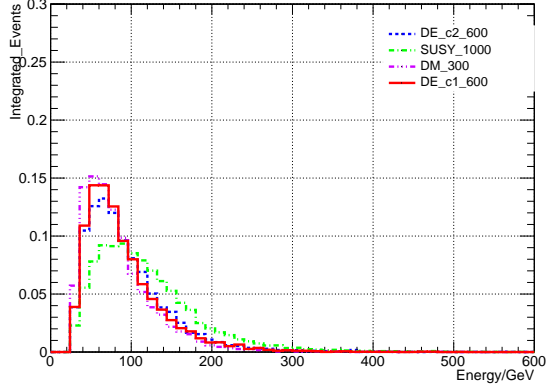Fig. 11.   Distributions preselection level.
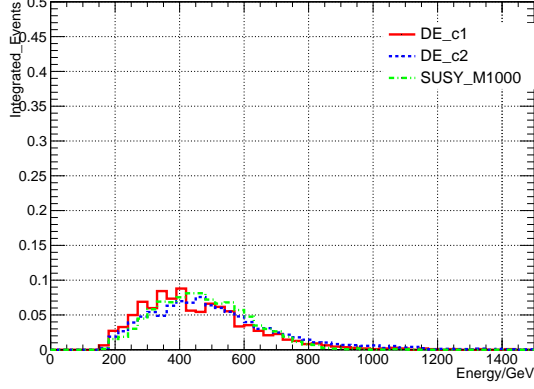
(a) amt2
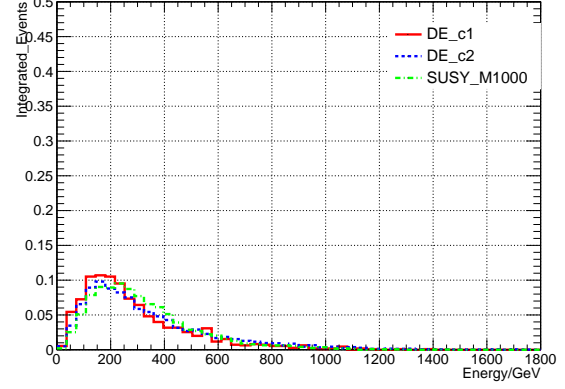
(b) bjet_pt
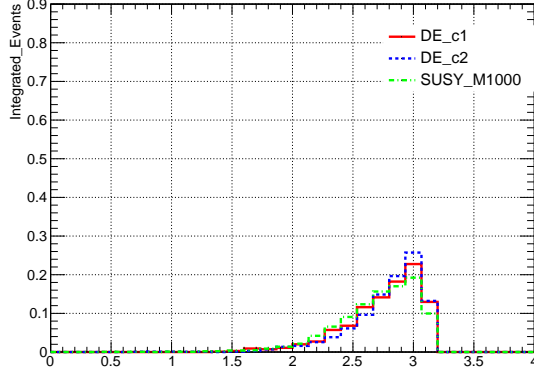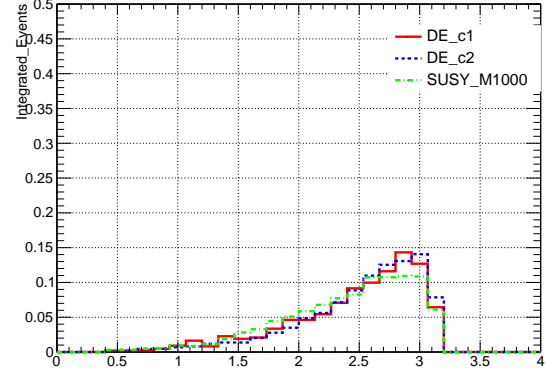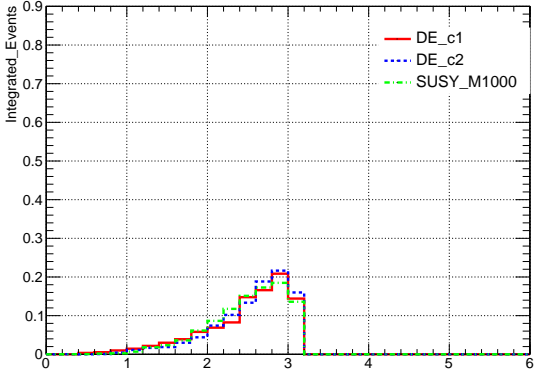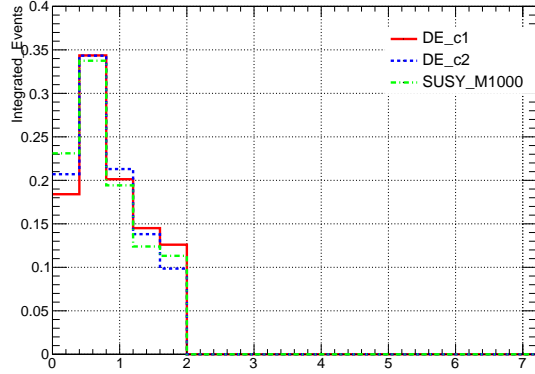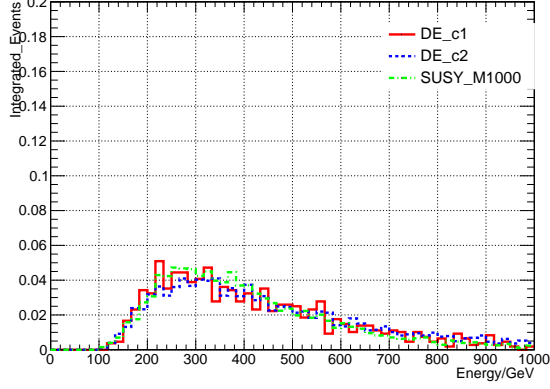
(c) dphi_jet0_ptmiss

(d) dphi_jet1_ptmiss

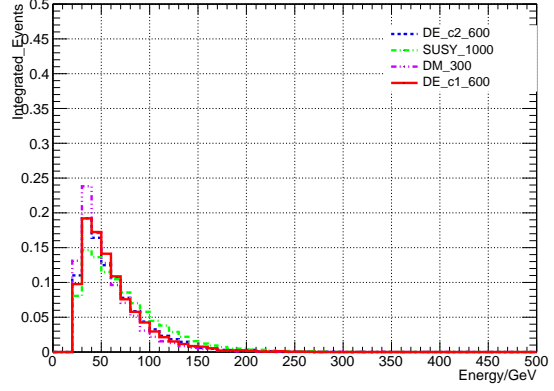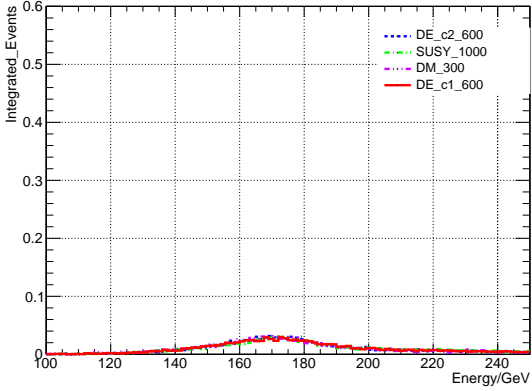(e) dphi_met_lep

(f) dr_bjet_lep
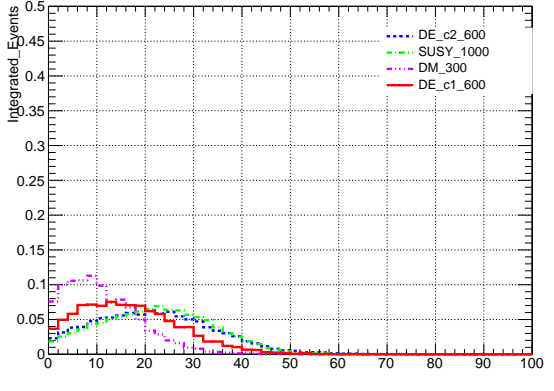
(g) leading_pt

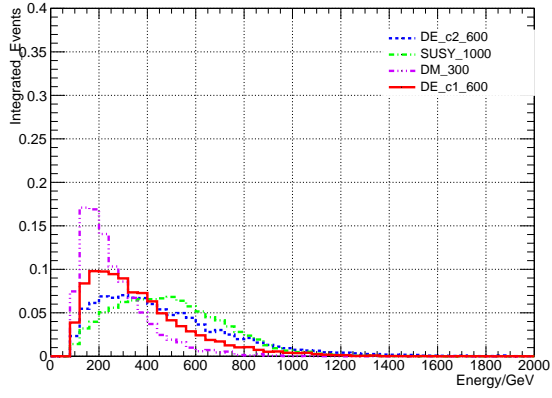(h) sub_leading_pt

(i) third_leading_pt

(j) fourth_leading_pt

(k) hadtop_mass

(l) ht_sig

(m) met

(n) mt
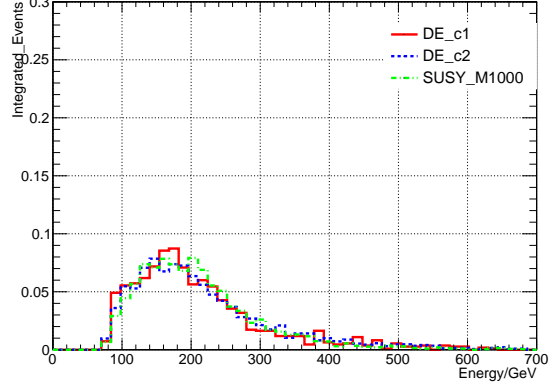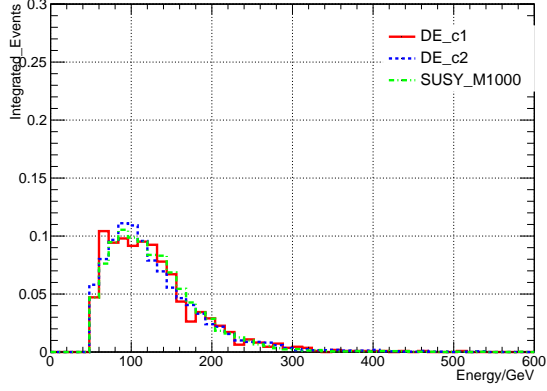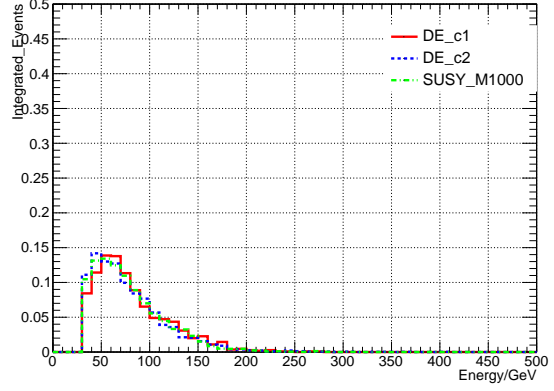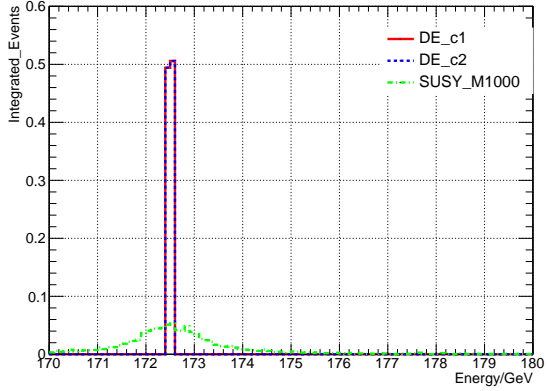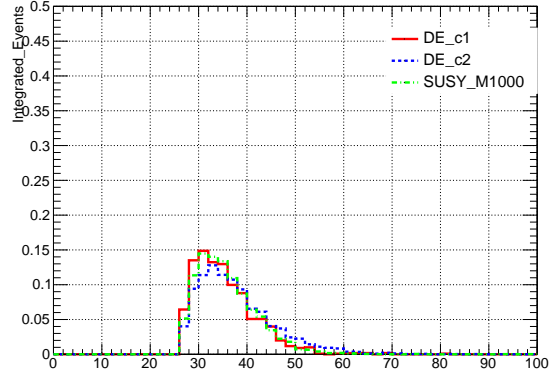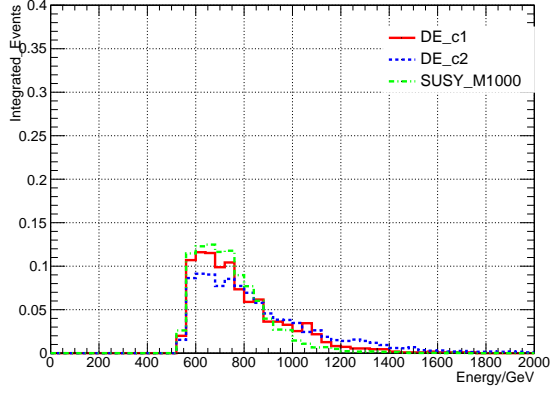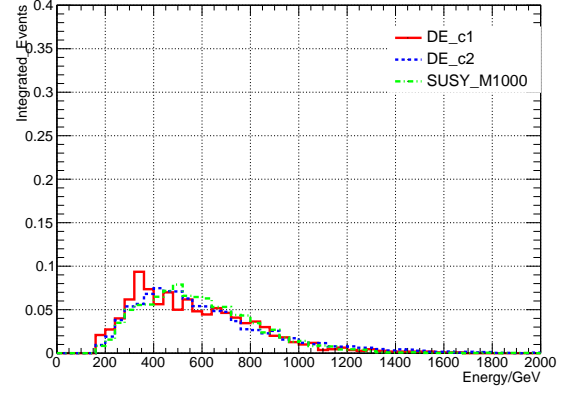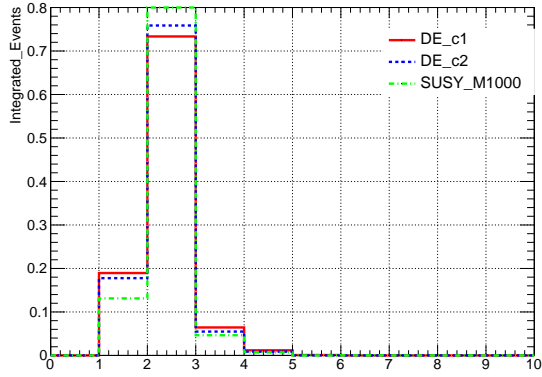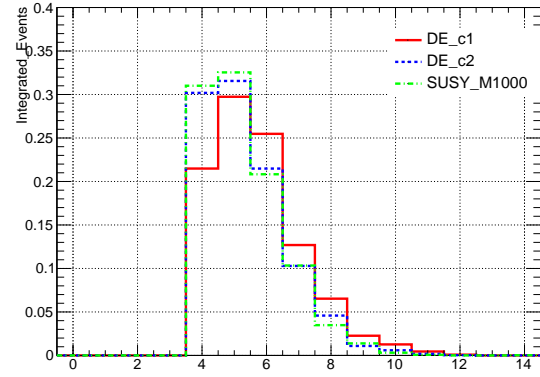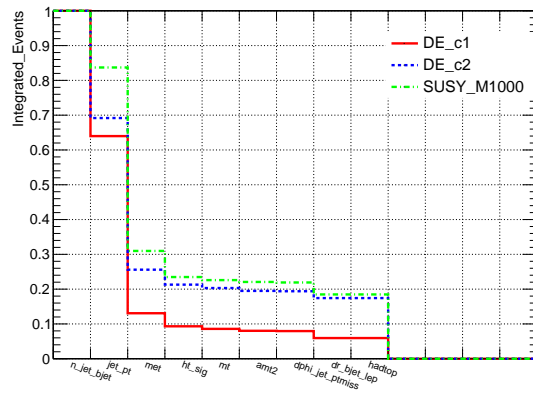
(o) n_bjet

(p) n_jet

(q) cut_efficiency

Fig. 12.   After tN_high selection.
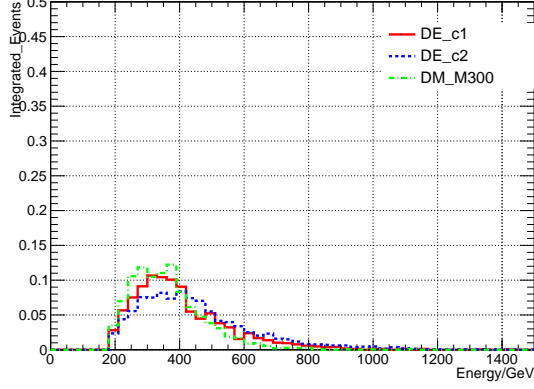
(a) amt2
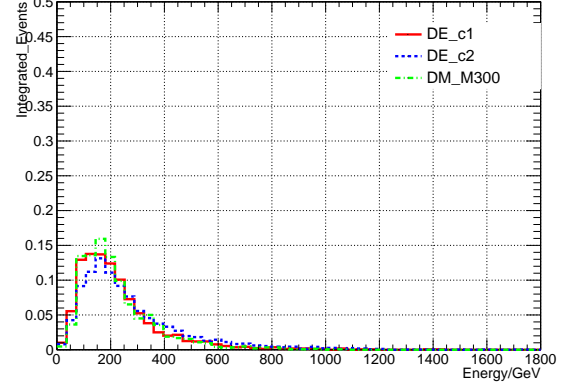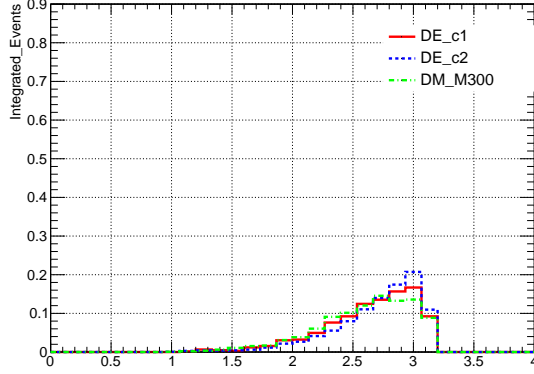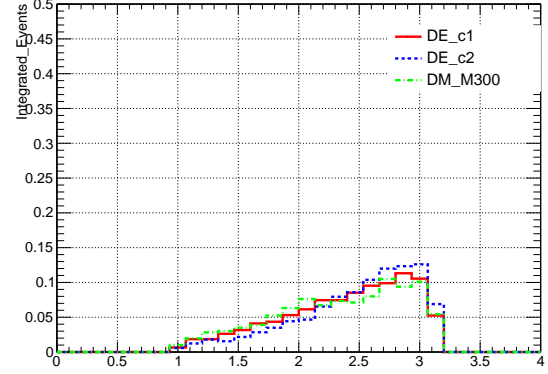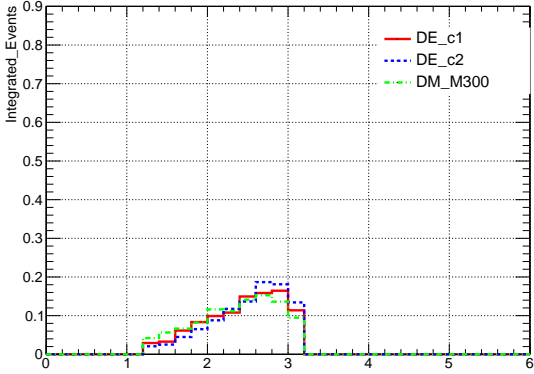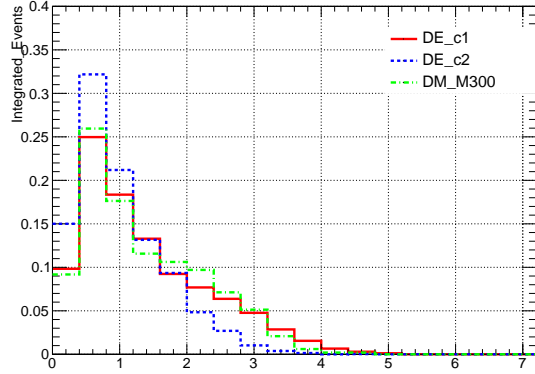
(b) bjet_pt

(c) dphi_jet0_ptmiss

(d) dphi_jet1_ptmiss

(e) dphi_met_lep

(f) dr_bjet_lep

(g) leading_pt
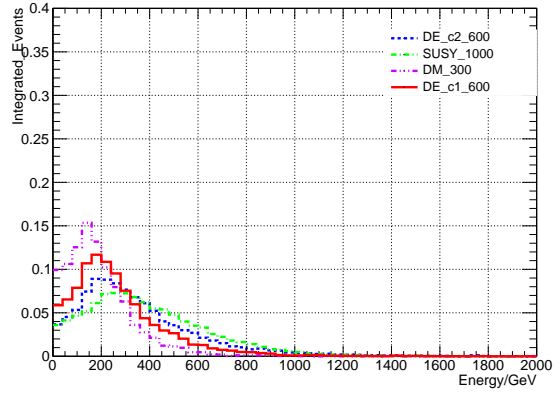

(h) sub_leading_pt
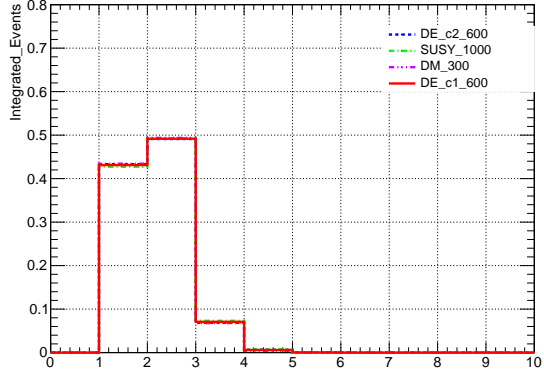

(i) third_leading_pt
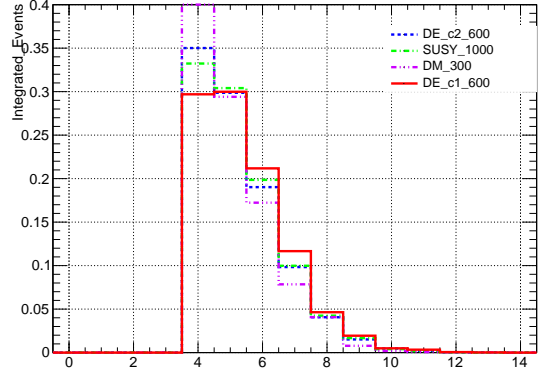

(j) fourth_leading_pt

(k) hadtop_mass

(l) ht_sig

(m) met

(n) mt
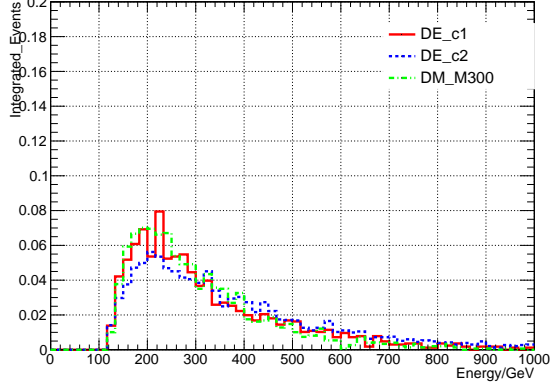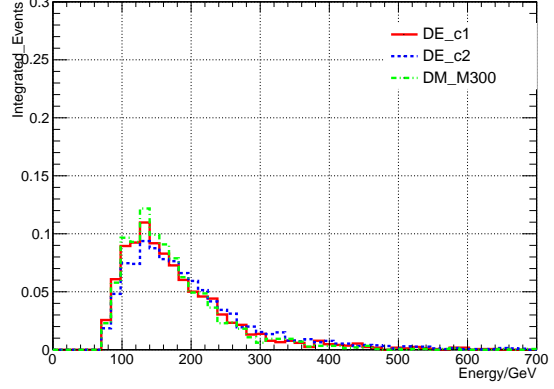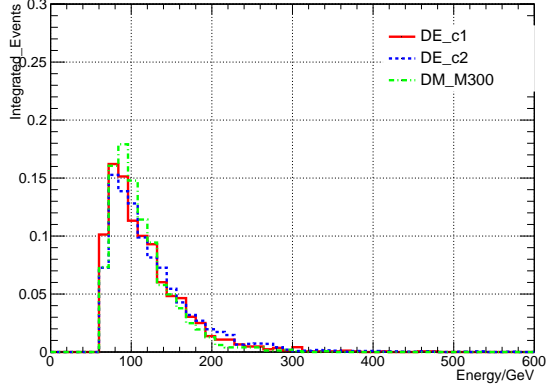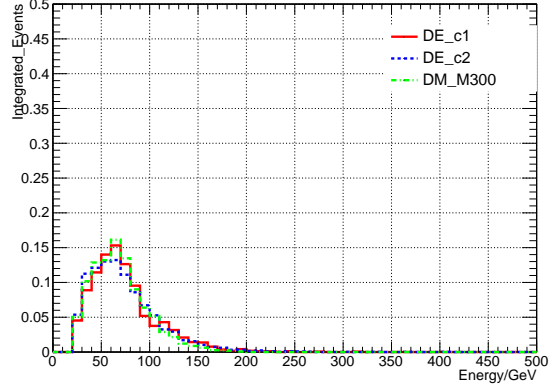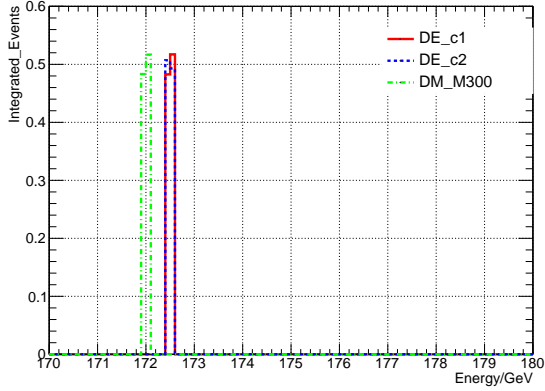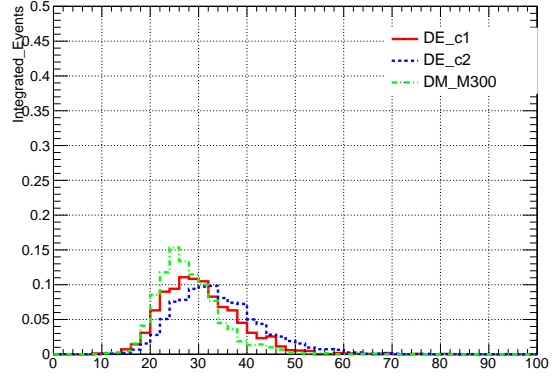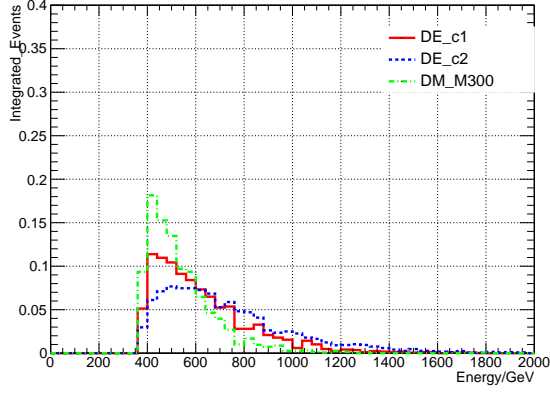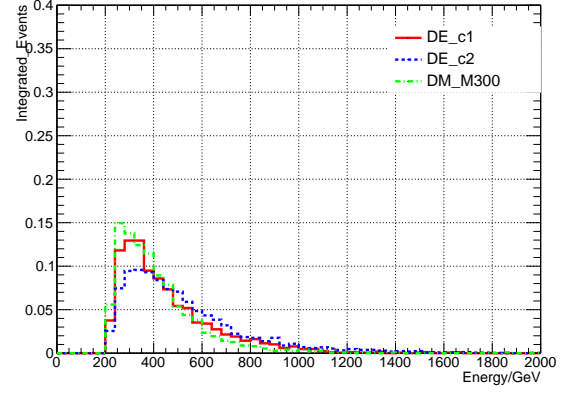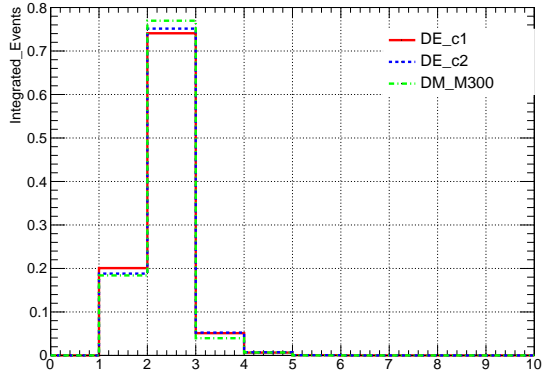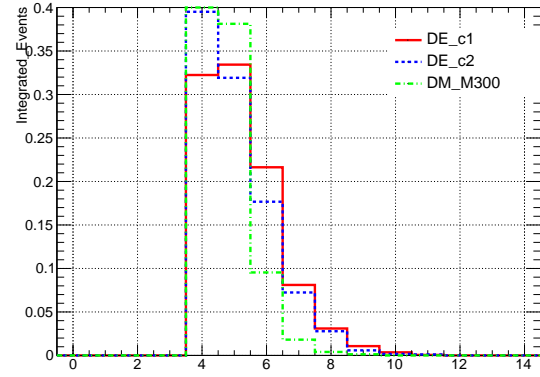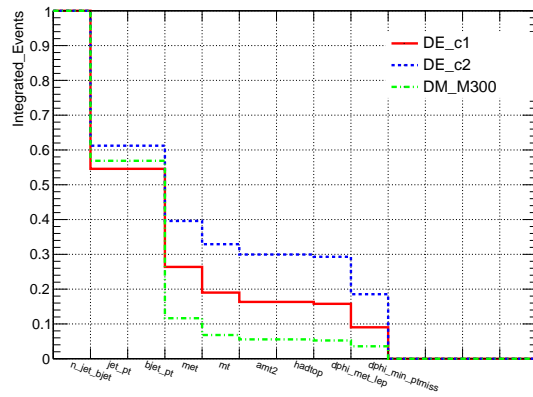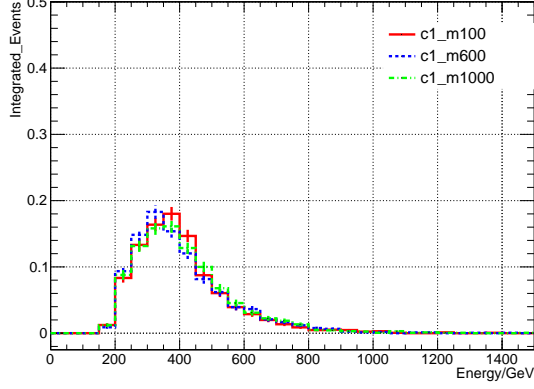

(o) n_bjet

(p) n_jet

(q) cut_efficiency

Fig. 13.   After DM_high selection.
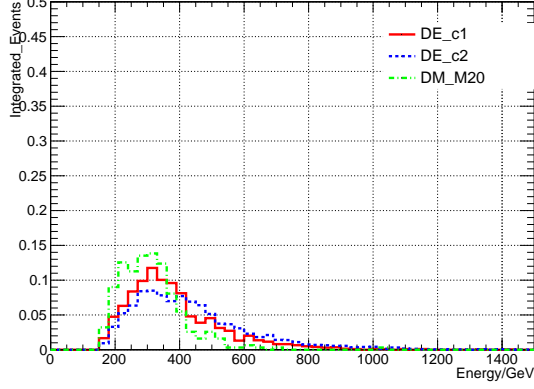
(a) amt2
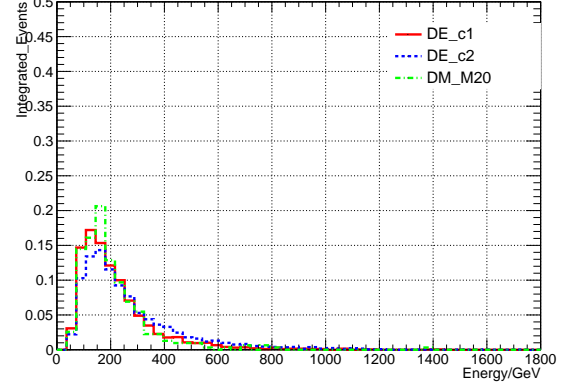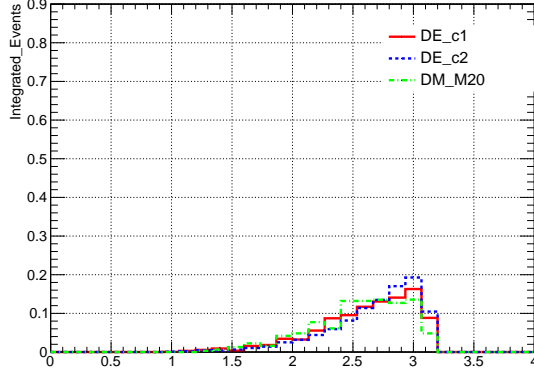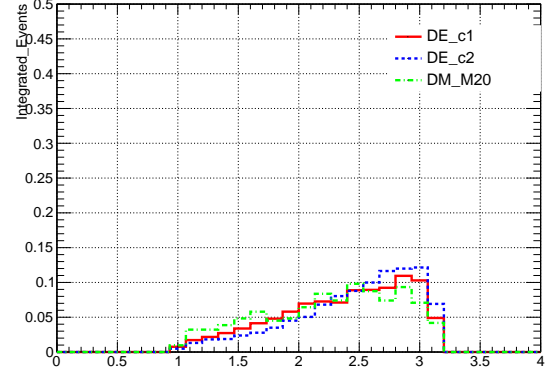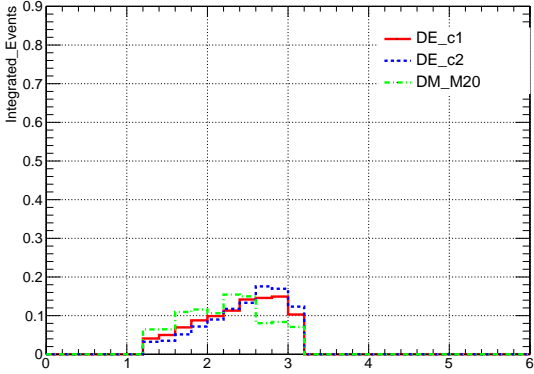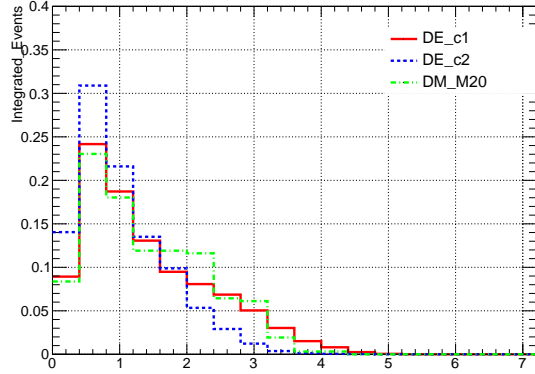
(b) bjet_pt

(c) dphi_jet0_ptmiss

(d) dphi_jet1_ptmiss

(e) dphi_met_lep

(f) dr_bjet_lep

(g) leading_pt

(h) sub_leading_pt

(i) third_leading_pt

(j) fourth_leading_pt

(k) hadtop_mass

(l) ht_sig

(m) met

(n) mt
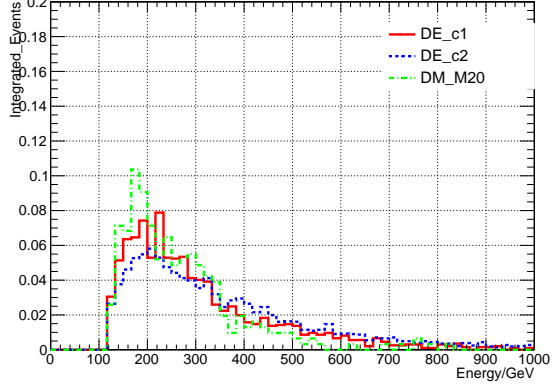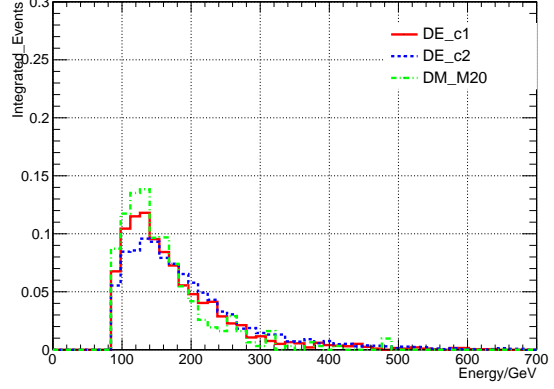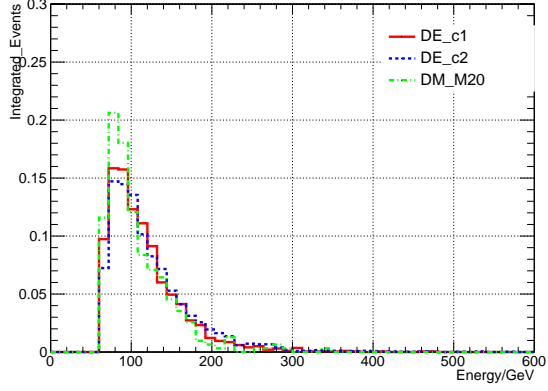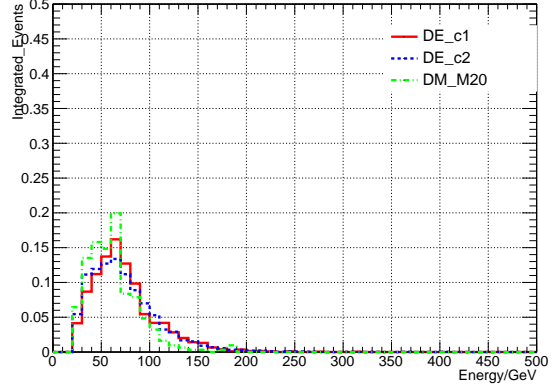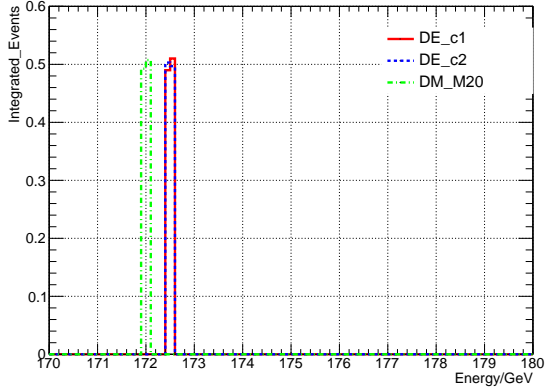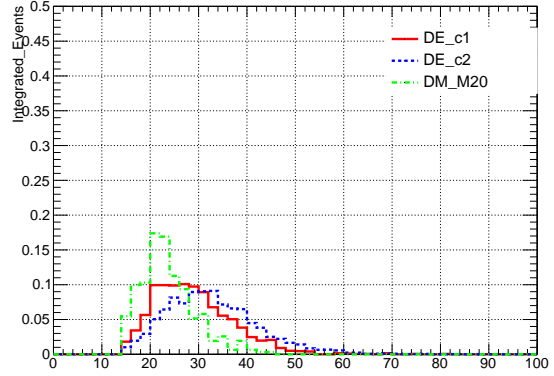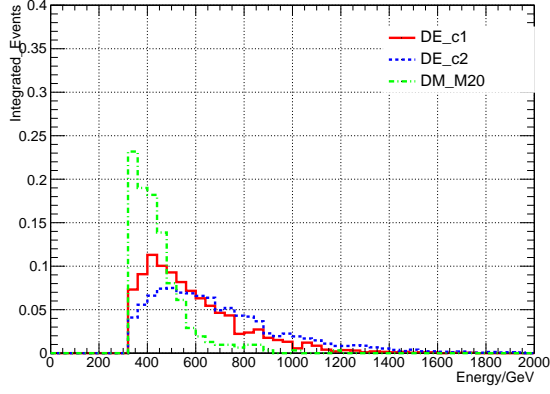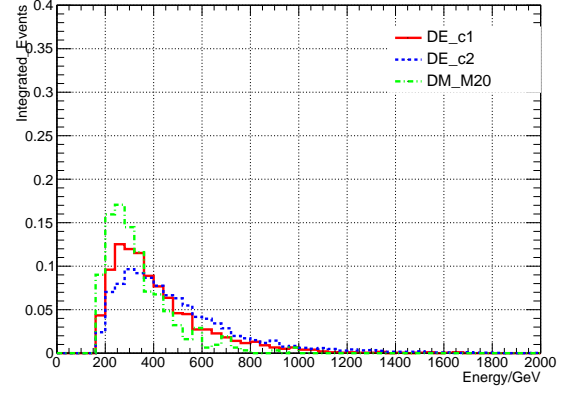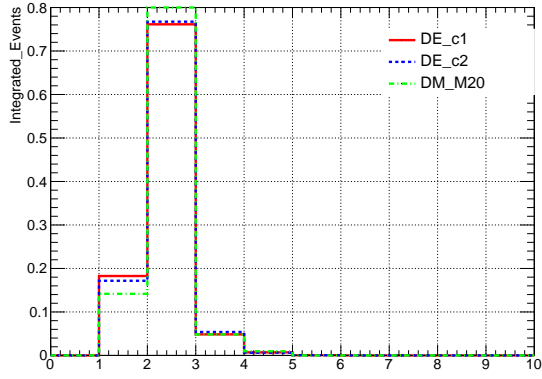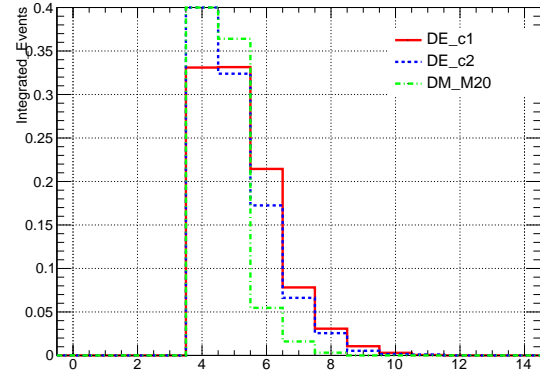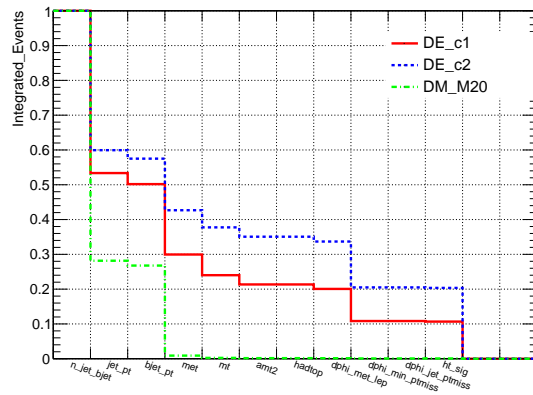
(o) n_bjet

(p) n_jet

(q) cut_efficiency
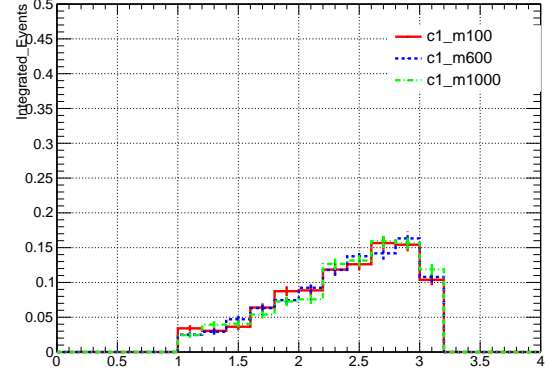
Fig. 14.   After DM_low selection.
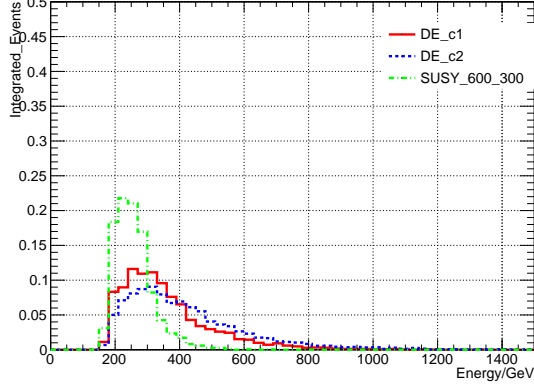
(a) amt2
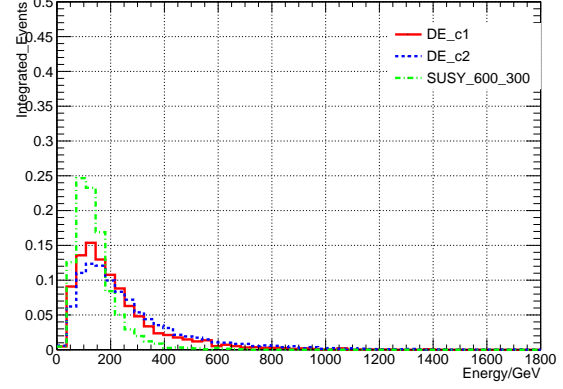
(b) bjet_pt
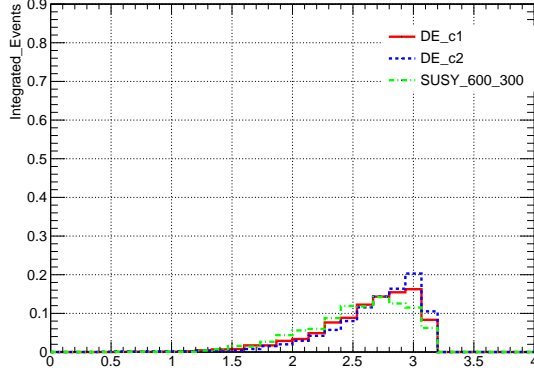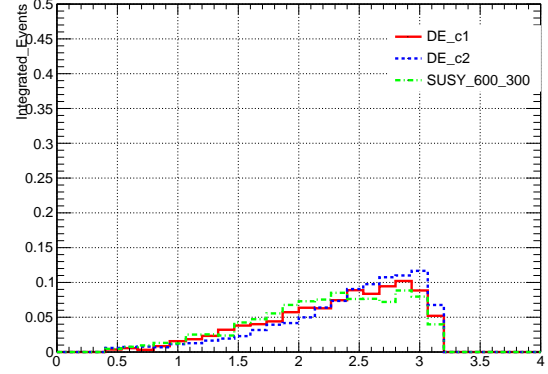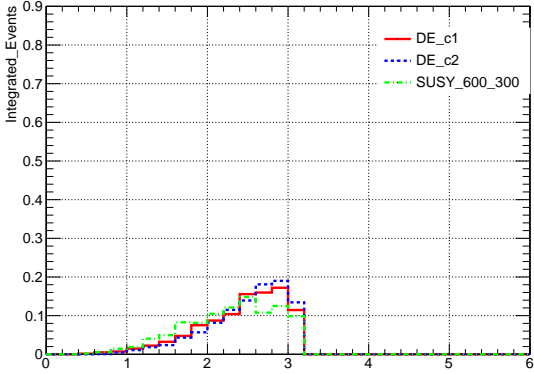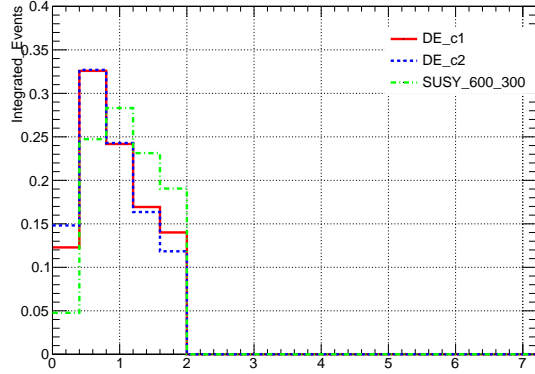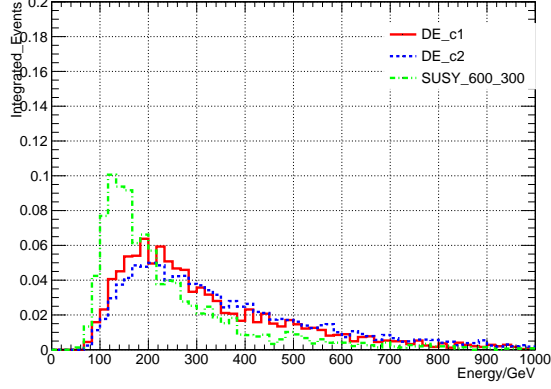
(c) dphi_jet0_ptmiss

(d) dphi_jet1_ptmiss

(e) dphi_met_lep

(f) dr_bjet_lep

(g) leading_pt

(h) sub_leading_pt

(i) third_leading_pt

(j) fourth_leading_pt

(k) hadtop_mass

(l) ht_sig

(m) met

(n) mt
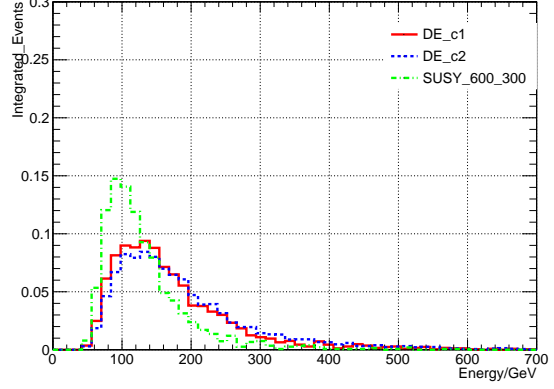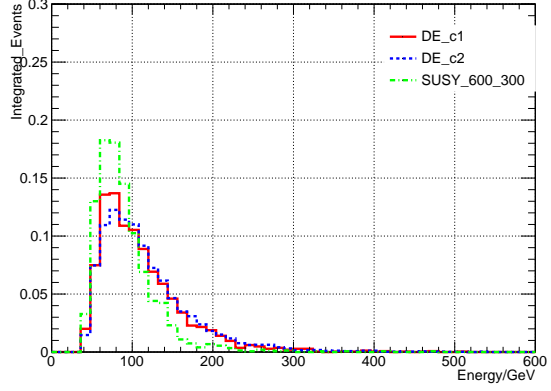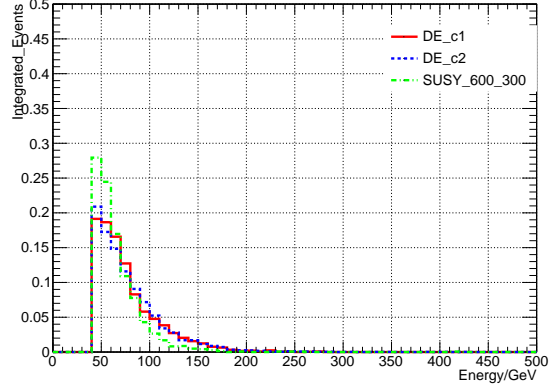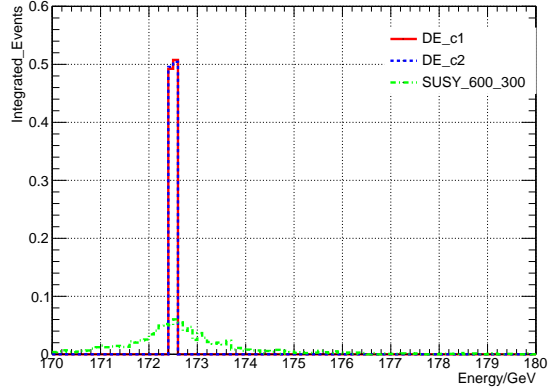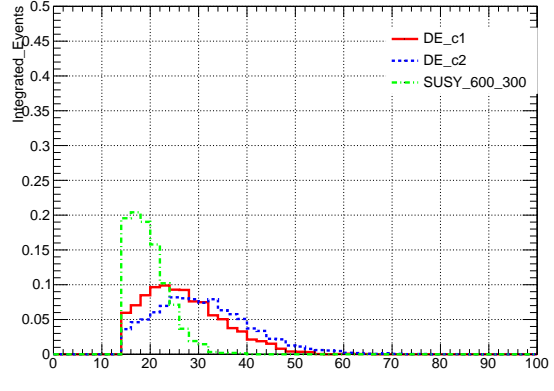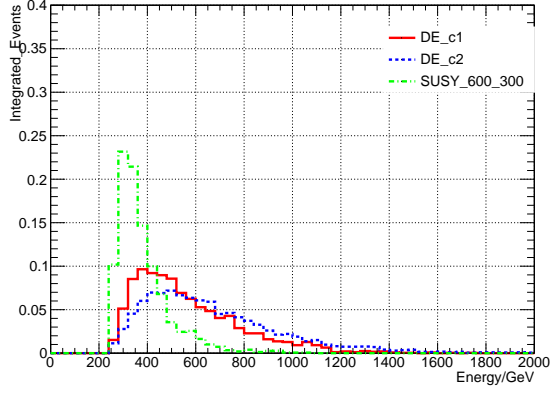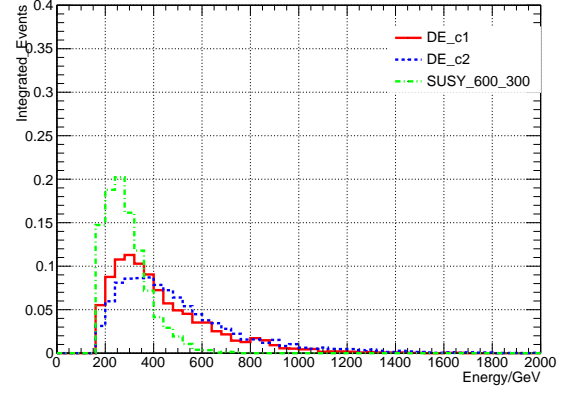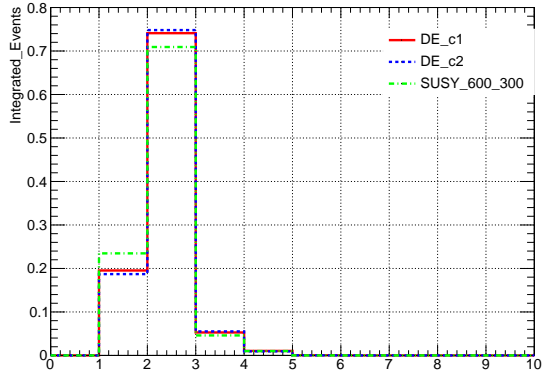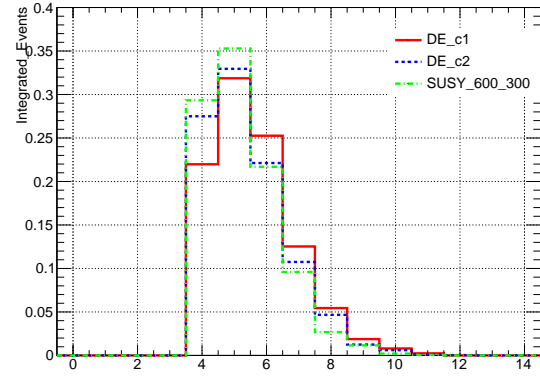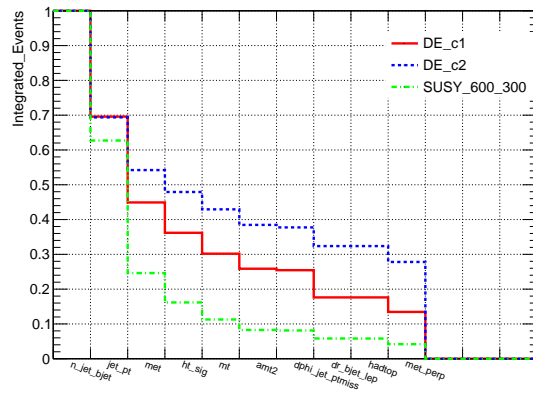
(o) n_bjet

(p) n_jet

(q) cut_efficiency

Fig. 15.　After tN_med selection.
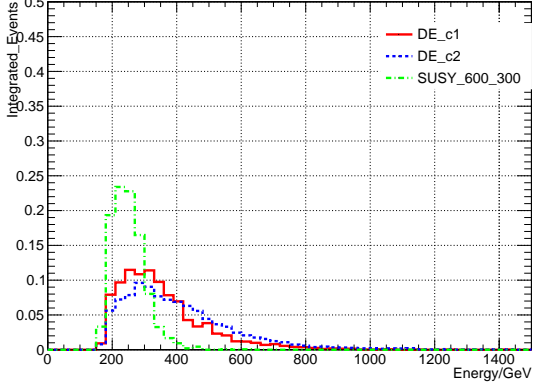
(a) amt2
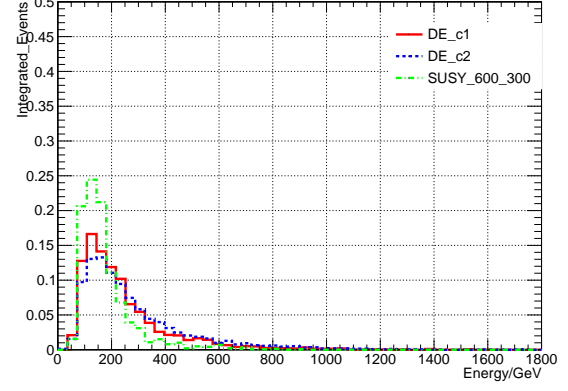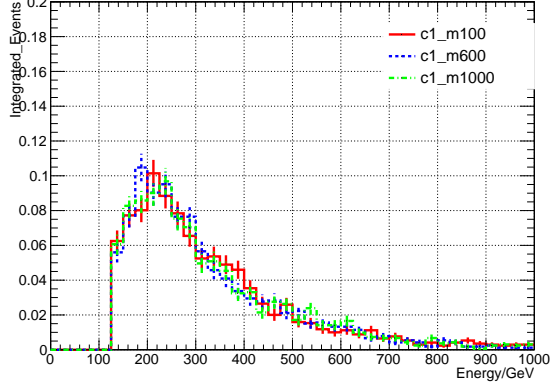

(b) bjet_pt
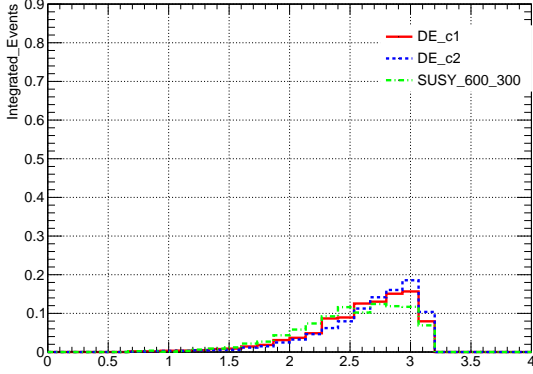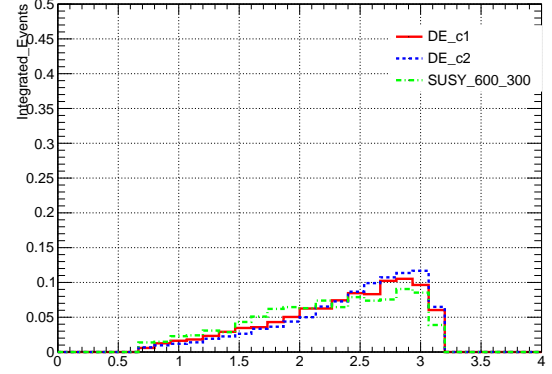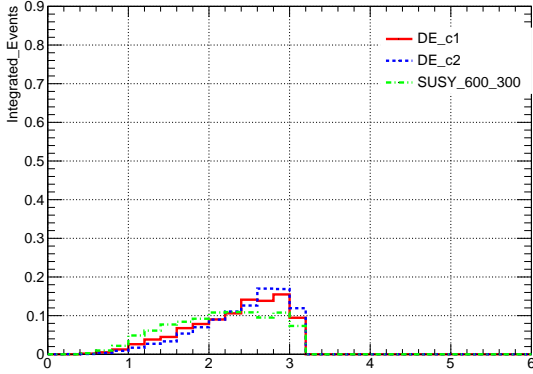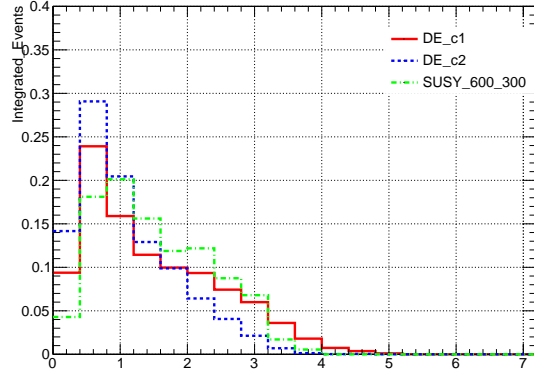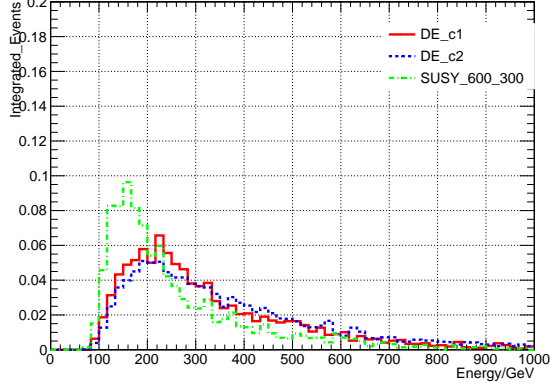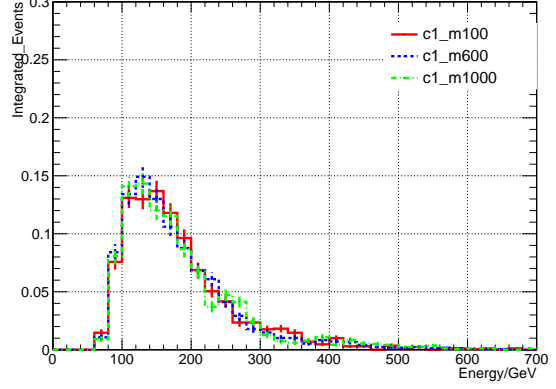

(c) dphi_jet0_ptmiss
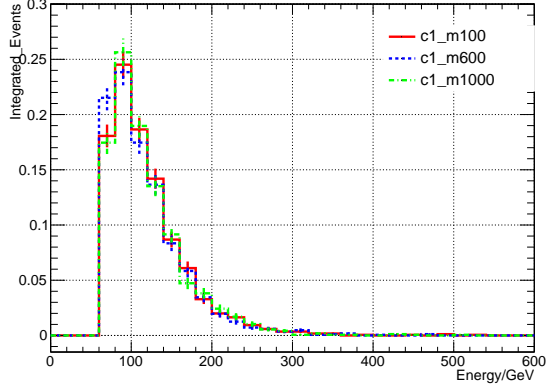

(d) dphi_jet1_ptmiss

(e) dphi_met_lep

(f) dr_bjet_lep

(g) leading_pt

(h) sub_leading_pt

(i) third_leading_pt

(j) fourth_leading_pt

(k) hadtop_mass

(l) ht_sig

(m) met

(n) mt
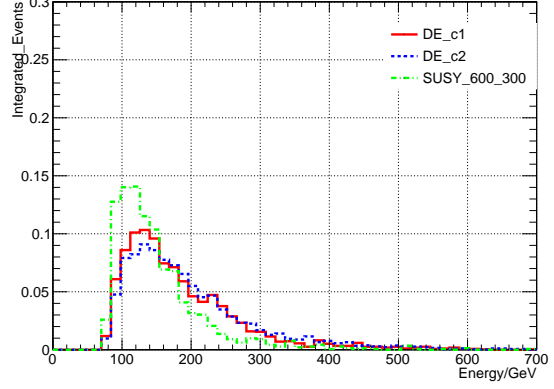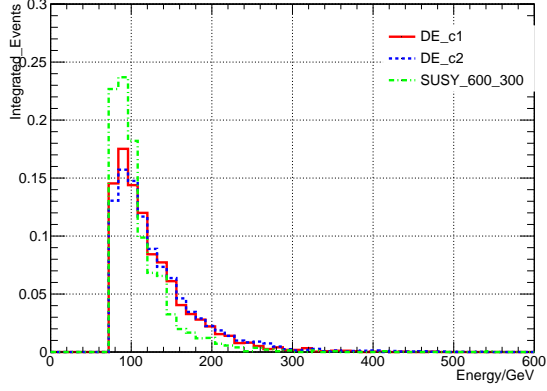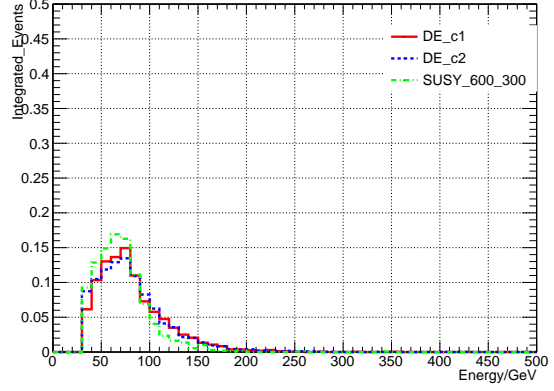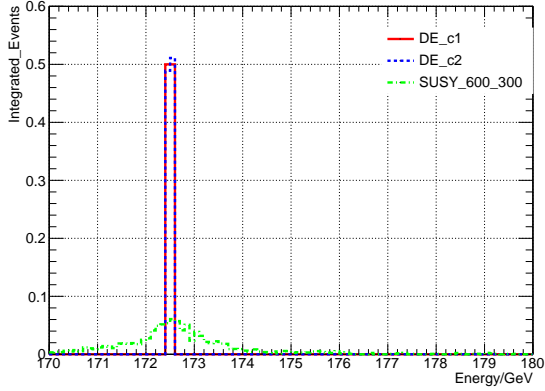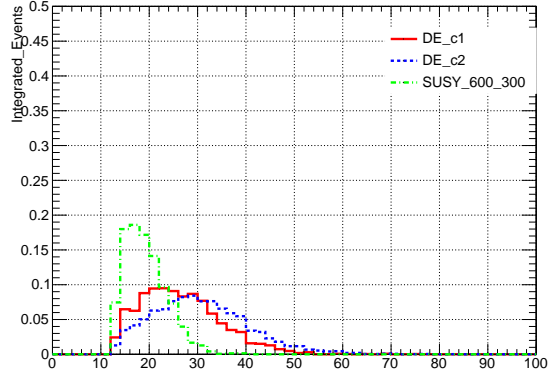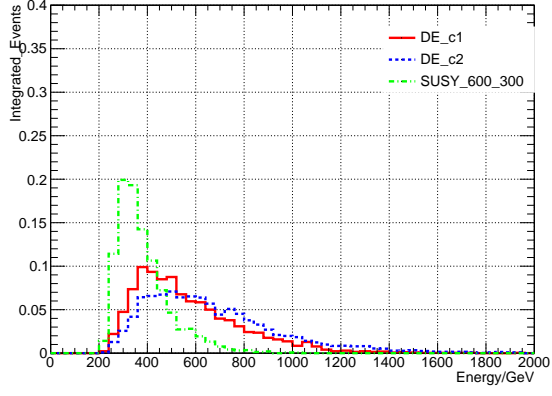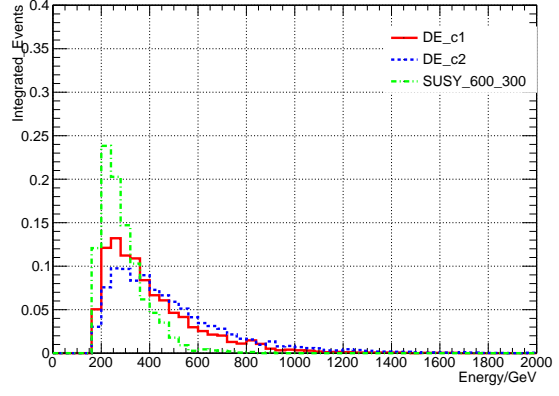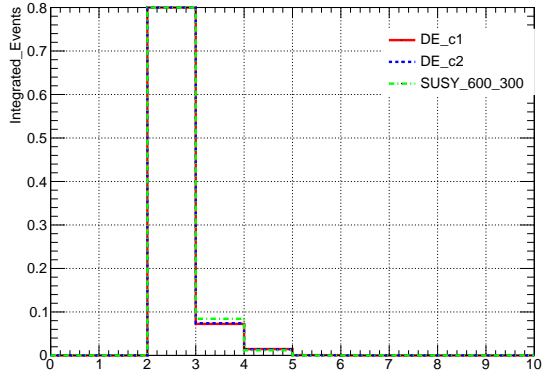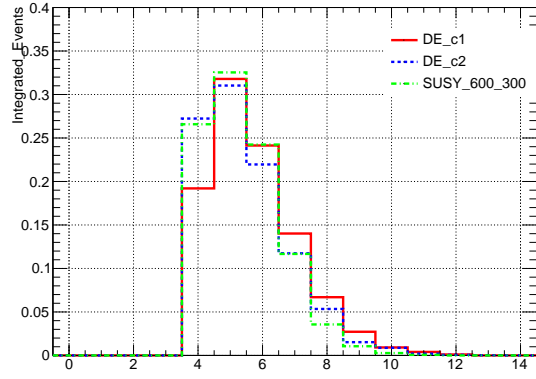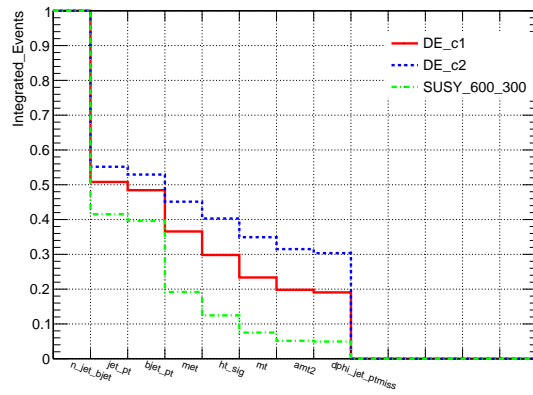
(o) n_bjet

(p) n_jet

(q) cut_efficiency

Fig. 16.   After bC2x_diag selection.
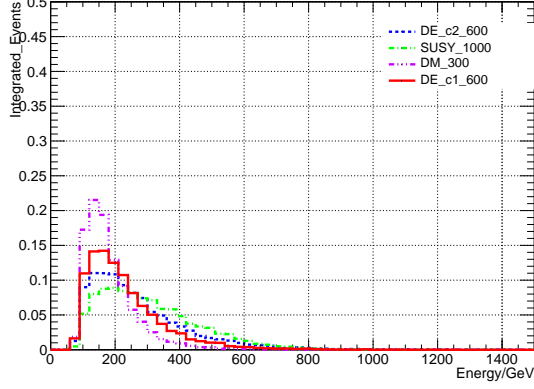
(a) amt2
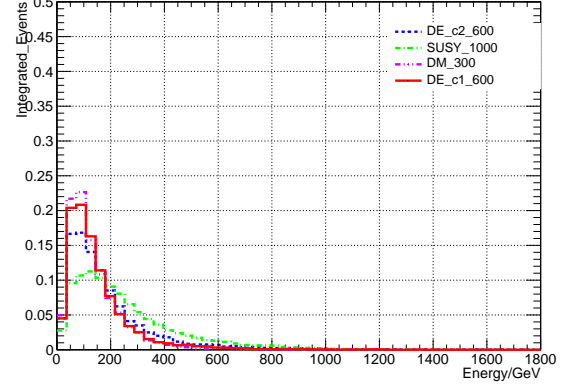
(b) bjet_pt
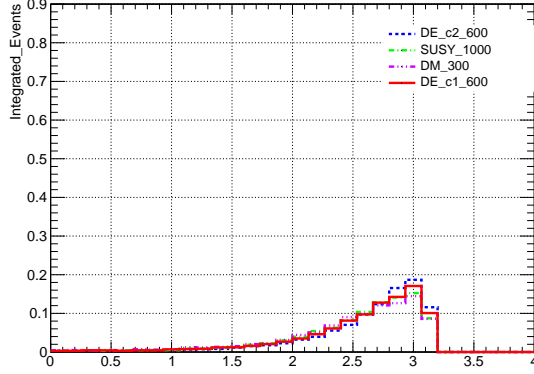
(c) dphi_jet0_ptmiss

(d) dphi_jet1_ptmiss
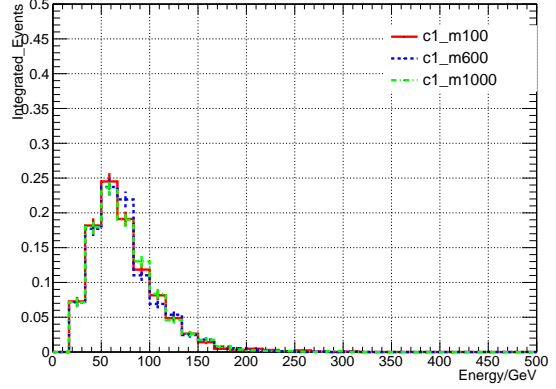

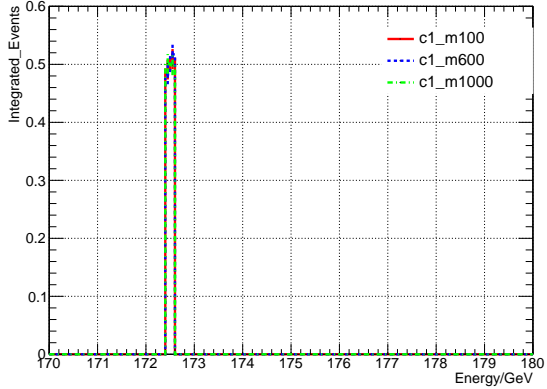(e) dphi_met_lep

(f) dr_bjet_lep
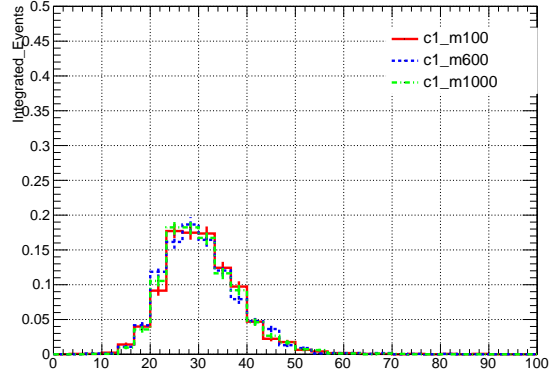
(g) leading_pt

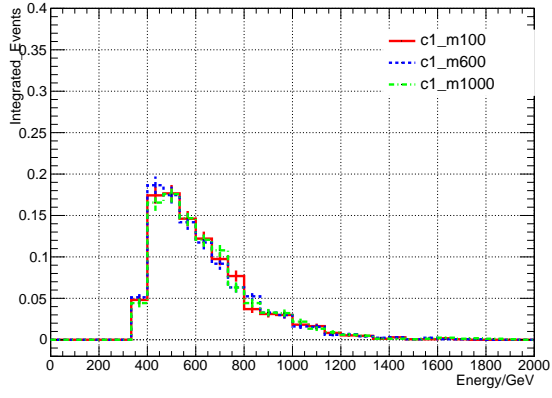(h) sub_leading_pt

(i) third_leading_pt

(j) fourth_leading_pt

(k) hadtop_mass

(l) ht_sig

(m) met

(n) mt

(o) n_bjet

(p) n_jet

Fig. 17. Distributions preselection at detector level.

(a) amt2
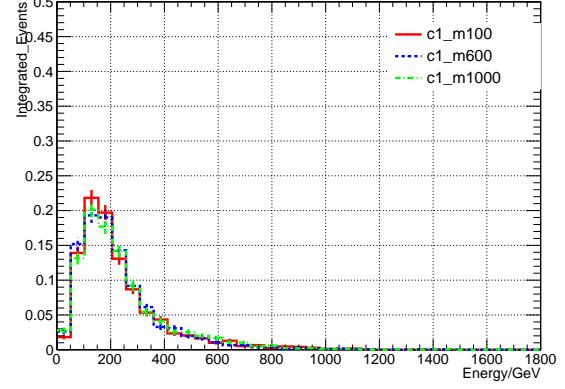
(b) bjet_pt
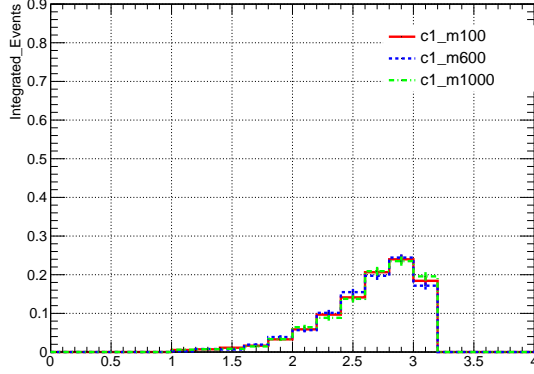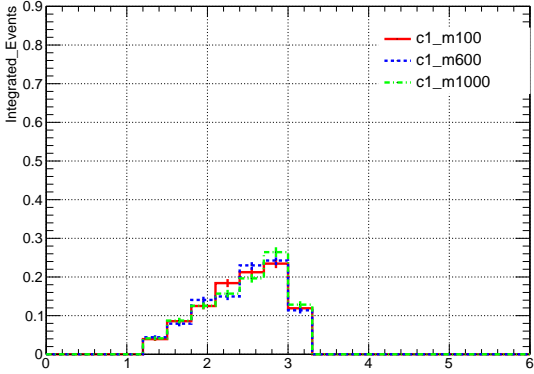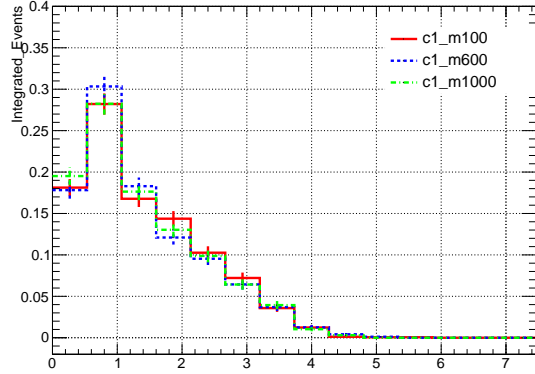
(c) dphi_jet0_ptmiss

(d) dphi_jet1_ptmiss

(e) dphi_met_lep

(f) dr_bjet_lep

(g) leading_pt

(h) sub_leading_pt

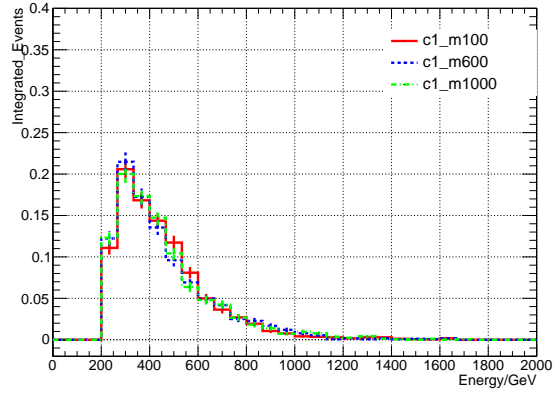(i) third_leading_pt
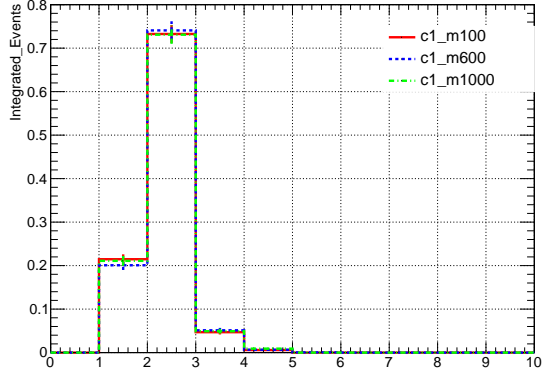

(j) fourth_leading_pt
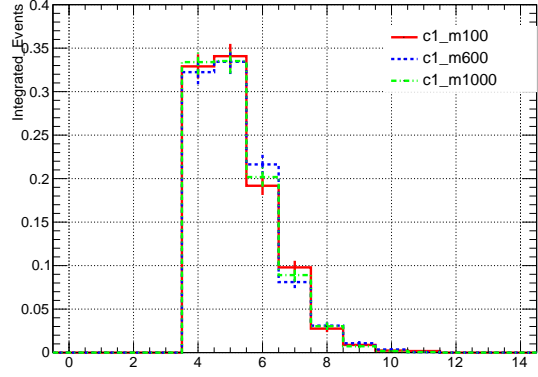

(k) hadtop_mass

(l) ht_sig

(m) met

(n) mt

(o) n_bjet

(p) n_jet

Fig. 18.   Distribution shapes at different M scales after DM_high selection.